MASTERARBEIT | MASTER'S THESIS

Titel | Title

Extraction of Microplastics from Compost: Fenton Reagent Optimisation for Efficient Organic Matrix Removal and Degradable Polymer Recovery.

verfasst von | submitted by

Julius Vincent Heinemann BSc

angestrebter akademischer Grad | in partial fulfilment of the requirements for the degree of

Master of Science (MSc)

Wien | Vienna, 2025

Studienkennzahl lt. Studienblatt | Degree programme code as it appears on the student record sheet:	UA 066 299
Studienrichtung lt. Studienblatt | Degree programme as it appears on the student record sheet:	Masterstudium Environmental Systems: Processes - Pollution - Solutions
Betreut von | Supervisor:	Univ.-Prof. Dr. Thilo Hofmann

Acknowledgements

I would like to thank everyone who supported me throughout the preparation of this master's thesis. First, I sincerely thank Univ.-Prof. Dr. Thilo Hofmann and Dr. Frank von der Kammer for the opportunity to work on this research project, for their expertise, guidance, and support throughout the process.

Special thanks to my mentor, Dean Velikov, for his valuable feedback, mentorship, and input, which greatly contributed to my work.

Thanks to Mariya Juric for her assistance with the carbon analyser and Mag. Peter Nagl for his introduction to the digital optical microscope. I would also like to thank the entire EDGE team for their support and for creating a welcoming and enjoyable working environment.

This thesis is part of the *"Development and Application of a Standardized Method for the Assessment of Microplastic Fragmentation in Compost"* project, a collaborative research effort between the University of Vienna and BASF SE (BASF). I am thankful to everyone involved in this initiative and to BASF for providing the materials and funding the entire project.

Finally, I appreciate the collective effort of all contributors to advancing sustainable and environmentally friendly practices.

Funding and Declaration of Competing Interest

This master's thesis was embedded in a project that received funding from BASF. The author declares that no known competing financial interests or personal relationships have influenced the work reported in this thesis.

Graphical Abstract

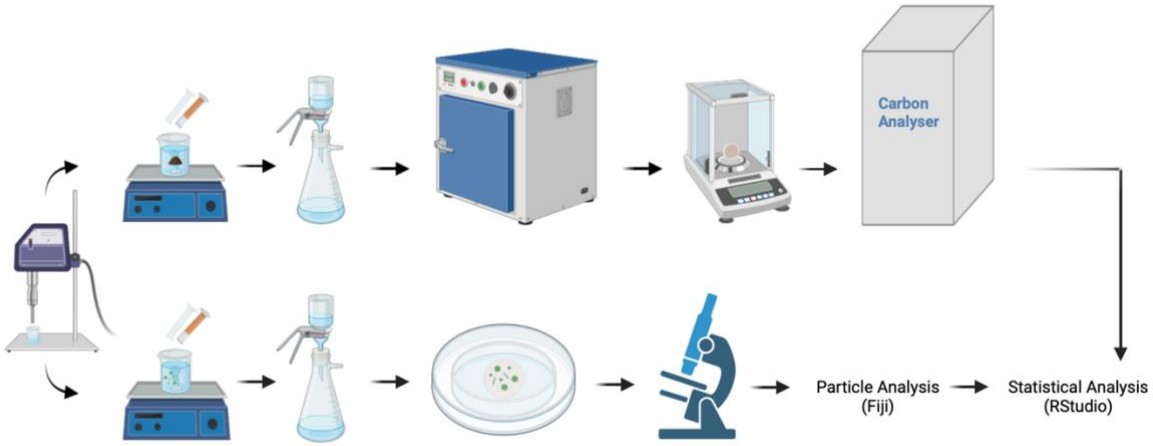

Created with biorender (https://www.biorender.com)

Abstract

Biodegradable plastics are a promising alternative to conventional, non-biodegradable fossil-fuel-based plastics, due to their potential environmental benefits. Biodegradable polymers are designed to undergo microbial metabolic utilisation, a process that converts their carbon content into carbon dioxide and microbial biomass. Although biodegradable polymers are developed to be ultimately completely mineralised, the process may also involve the transient formation of ever-smaller fragments. A better understanding of their behaviour, degradation rates, particle sizes and the development of a standardised microplastic extraction method is key to improving knowledge of biodegradation kinetics. This study aimed to improve the efficiency, cost-effectiveness, and recovery rates of extracting degradable plastics from compost, specifically polylactic acid and polybutylene adipate-co-terephthalate. To achieve this, we optimised the Fenton reagent method for organic matter removal while minimising damage to the polymers. Different concentrations of hydrogen peroxide and iron catalyst were tested. We measured mass loss and total organic carbon removal, comparing results to untreated controls. The optimised protocol achieved an average organic carbon removal of 82.53% ± 6.64% while keeping temperatures below 50 °C during the reaction. The impact on polylactic acid and polybutylene adipate-co-terephthalate particles was assessed using digital optical microscopy and particle analysis in Fiji, followed by a statistical evaluation in RStudio. A slight reduction in particle size was observed, however, no statistically significant differences in particle size distribution were found between pre- and post-treatment samples. Compared to previous protocols, the presented method significantly reduces processing time and ensures reproducibility. This scalable, cost- and time-effective solution supports the development and usage of biodegradable polymers, and environmental monitoring.

Kurzfassung

Biologisch abbaubare Kunststoffe sind eine vielversprechende Alternative zu konventionellen, nicht biologisch abbaubaren Kunststoffen auf fossiler Basis, da sie potenzielle Umweltvorteile bieten. Biologisch abbaubare Polymere sind so konzipiert, dass sie durch mikrobielle Stoffwechselprozesse abgebaut werden, bei denen ihr Kohlenstoffgehalt in Kohlenstoffdioxid und mikrobielle Biomasse umgewandelt wird. Obwohl biologisch abbaubare Polymere entwickelt wurden, um vollständig mineralisiert zu werden, kann der Prozess auch zur vorübergehenden Bildung immer kleinerer Fragmente führen. Ein besseres Verständnis ihres Verhaltens, ihrer Abbauraten, Partikelgrößen sowie die Entwicklung einer standardisierten Methode zur Mikroplastikextraktion ist entscheidend, um das Wissen über die Kinetik des Abbaus zu verbessern. Ziel dieser Studie war es, die Effizienz, Kosteneffektivität und Rückgewinnungsraten bei der Extraktion biologisch abbaubarer Kunststoffe aus Kompost, insbesondere Polylactid und Polybutylen(adipat-co-terephthalat), zu verbessern. Dazu wurde die Fenton-Reagenz-Methode zur Entfernung der organischen Matrix optimiert, um Schäden an den Polymeren zu minimieren. Verschiedene Konzentrationen von Wasserstoffperoxid und Eisenkatalysator wurden getestet. Der Massenverlust und die Entfernung des organischen Kohlenstoffs wurden gemessen und mit unbehandelten Kontrollproben verglichen. Das optimierte Protokoll erzielte eine durchschnittliche Entfernung von organischem Kohlenstoff von 82.53% ± 6.64%, wobei die Reaktionstemperaturen unter 50 °C gehalten wurden. Die Auswirkungen auf Polylactid- und Polybutylen(adipat-co-terephthalat)-Partikel wurden mittels digitaler optischer Mikroskopie und Partikelanalyse in Fiji untersucht, gefolgt von einer statistischen Auswertung in RStudio. Es wurde eine leichte Reduktion der Partikelgröße beobachtet, jedoch keine statistisch signifikanten Unterschiede in der Partikelgrößenverteilung zwischen den Proben vor und nach der Behandlung festgestellt. Im Vergleich zu früheren Protokollen reduziert die hier vorgestellte Methode die Prozessdauer erheblich und gewährleistet Reproduzierbarkeit. Diese skalierbare, kosten- und zeiteffiziente Lösung unterstützt die Entwicklung und Verwendung biologisch abbaubarer Polymere sowie das Umweltmonitoring.

Table of Contents

ACKNOWLEDGEMENTS ..... **III**

GRAPHICAL ABSTRACT ..... **IV**

ABSTRACT ..... **V**

KURZFASSUNG ..... **VI**

1 INTRODUCTION **1**

2 STATE OF KNOWLEDGE **4**

2.1 Plastics and Microplastics 4
2.1.1 Polylactic Acid and Polybutylene Adipate-co-Terephthalate *5*
2.1.2 Biodegradability *8*
2.2 Compost 9
2.2.1 Production and Use of Compost *9*
2.2.2 Regulations in Austria and Germany *11*
2.2.3 Plastic Found in Compost *12*
2.3 Extraction Methodologies of Plastics 13
2.4 Fenton Reaction 14
2.5 Microplastics Analysis Techniques 15

3 AIMS & HYPOTHESES **17**

4 MATERIALS & METHODS **19**

4.1 Organic Matrix Removal 19
4.1.1 Organic Matrix Removal by Fenton Oxidation *19*
4.1.2 Organic Matrix Removal by Sodium Hypochlorite *23*
4.2 Carbon Analysis 24
4.2.1 Determination of the Combustible Fraction Using Loss-on-Ignition and Carbon Analyser *24*
4.2.2 Total Organic Carbon Analysis *25*
4.3 Polymer Size and Morphology Analysis 27
4.3.1 Fenton Oxidation and Filter Process *27*
4.3.2 Digital Optical Microscopy and Particle Analysis *28*
4.4 Statistics 30

5 RESULTS & DISCUSSION **32**

5.1 Effect of Different Fenton Reagent Conditions on the Degradation Efficiency of Organic Matter in Compost 32
5.1.1 Mass Loss Analysis *33*
5.1.2 Total Organic Carbon Analysis *38*
5.2 Combustible Fraction of Native Compost 42
5.3 Impact of the Optimised Fenton Protocol on the Integrity of Biodegradable Polymers 43

6 CONCLUSIONS AND ENVIRONMENTAL IMPLICATIONS **48**

7 REFERENCES **50**

APPENDIX ..... **A**

SUPPLEMENTARY INFORMATION ..... **D**

1 Introduction

Plastic pollution remains one of the most pressing environmental issues, contributing to long-term ecological damage [1]. Plastics are among the most widely used and produced materials globally, with production reaching over 400 million metric tons in 2022 [2]. It is well documented that plastics contaminate every environmental compartment, including terrestrial, marine and freshwater ecosystems, and, as has been recently proven, also the atmosphere [3]. Even under the most optimistic predictions, annual plastic emissions are estimated to reach 53 million metric tons entering aquatic ecosystems by 2030 [4]. Plastics can be classified into four major types based on their origin and degradability: Non-biodegradable and fossil-fuel based, non-biodegradable and renewable-sources based, biodegradable and fossil-fuel based, and biodegradable and renewable-sources based (Fig. 1).

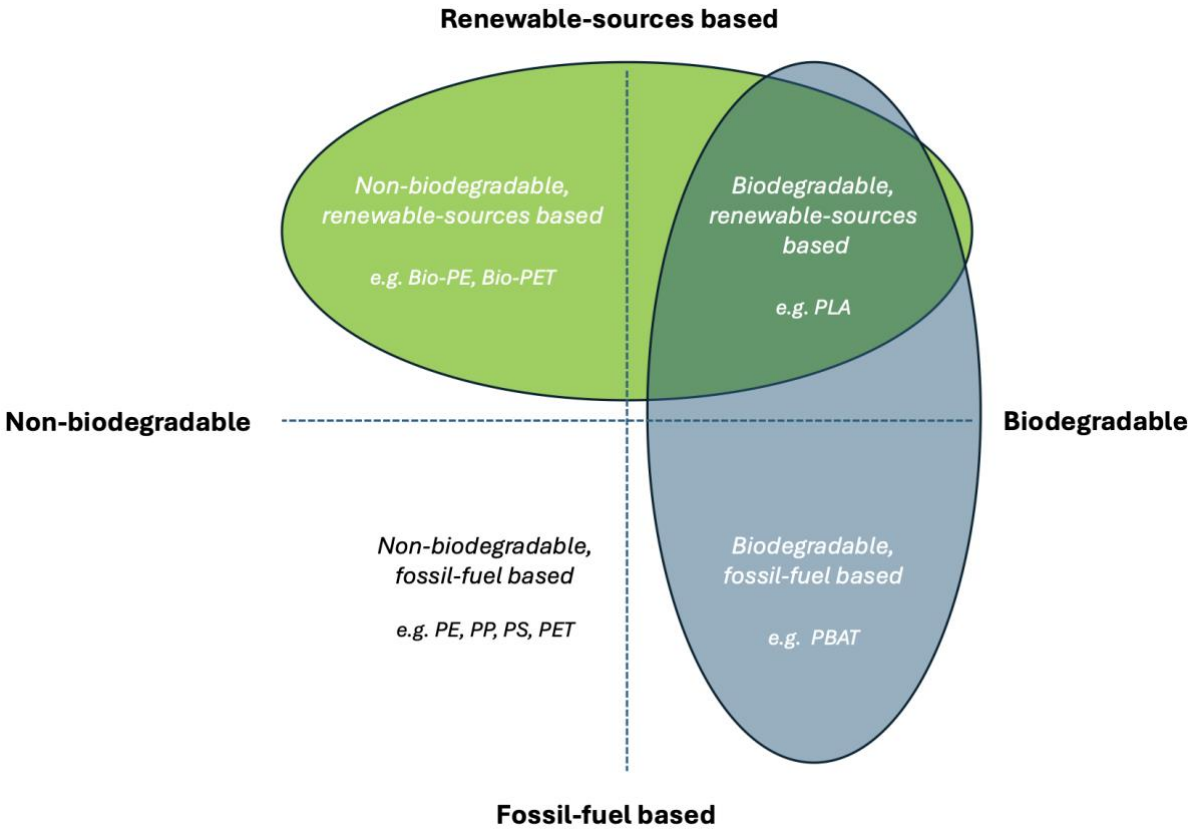

Figure 1: Major types of plastics based on their origin and degradability.

Non-biodegradable, fossil-fuel based plastics, commonly known as “conventional” plastics, are typically environmentally persistent [5], [6]. They are highly resistant to degradation, persisting in ecosystems and might fragment into persistent microplastics (MPs) [7]. Once emitted to the environment, such MPs can be ingested and inhaled by organisms, with the potential to accumulate in different tissues [1], [8]. Through the food chain, MPs may also enter the human body, they have been detected, for example, in human placentas [9] and lungs [10], as well as other organs [11].

Although it is currently unclear to what extend plastics pose a risk to both humans and livestock [12], it is concerned that, regardless of their own potential toxicity, they may additionally be able to transport other pollutants through different environments. A recent study has shown that although the desorption of most organic pollutants is too fast for MPs to act as transport agents in soil, very hydrophobic organic pollutants ($\log K_{ow}$ >5) could lead to transfer and translocation of these substances in the environment under preferential flow conditions [13].

Despite numerous uncertainties, one fact remains clear: plastics are persistent and do not disappear; they are transported across environments and accumulate over time. While the utility and advantages of plastics are undeniable, so too are the environmental damages they may cause.

In response to these issues, biodegradable plastics have been developed, offering the potential for degradation under specific conditions, representing a promising alternative [14], [15]. They demonstrate significant potential in supporting global efforts toward a sustainable circular economy and the reduction of plastic waste.

In the context of a circular economy, compost holds significant potential. By transforming organic waste into a valuable resource, composting reduces the need for landfilling and promotes sustainable waste management [16]. Compost enriches soil by increasing soil organic matter, which improves soil structure [17], water retention, and erosion prevention, essential for long-term soil health [18]. It enhances nutrient availability, reducing reliance on chemical fertilisers and promoting natural fertility cycles [19]. Additionally, it supports soil biodiversity and suppresses soil-borne

diseases [20], fostering healthier ecosystems and improving crop yields [16], making it an effective tool for sustainable agriculture and resource recovery.

However, since compost is seen as a benefitable material used in gardening and agriculture, the presence of persistent MPs is of concern. For this reason, fully biodegradable plastics may play a particularly important role in compost and waste collection systems. Biodegradable plastics permitted in organic waste collections must degrade in industrial composting facilities to avoid contaminating agricultural fields.

Despite their promise, extracting and analysing biodegradable plastics from complex, organic-rich matrices, such as compost or environmental samples, remains challenging. Harsh extraction methods may compromise particle integrity [21], [22], complicating their analysis. To accurately assess the environmental impact of biodegradable plastics, standardised analytical techniques must be developed.

This study examines current extraction protocols and seeks to optimise existing methods. It focuses on the degradation of organic matter through Fenton oxidation and its impact on the structural integrity of key biodegradable polymers, such as polylactic acid (PLA) and polybutylene adipate-co-terephthalate (PBAT). By improving these extraction methods, the study not only advances the technical understanding of biodegradable plastic degradation but also addresses broader sustainability challenges linked to global environmental goals.

The increasing use of biodegradable plastics and research on their degradation align with several United Nations Sustainable Development Goals (SDGs). This study supports global sustainability efforts by optimising extraction protocols, contributing to SDG 12 (Responsible Consumption and Production) by promoting sustainable production cycles, SDG 14 (Life Below Water) by addressing plastic pollution in marine ecosystems, and SDG 13 (Climate Action) by reducing carbon emissions through the replacement of conventional plastics. Additionally, the research advances innovation and sustainable infrastructure in materials science, supporting SDG 9 (Industry, Innovation, and Infrastructure) [23].

2 State of Knowledge

2.1 Plastics and Microplastics

Plastics, a class of synthetic polymers, serve as a hallmark of the Anthropocene. Fossils mark the emergence of different life forms; similarly, the presence of plastics in the geological record will reflect humanity's rise to global dominance.

Plastics are artificially synthesized materials consisting of one or more organic polymers combined with additives to achieve specific functional properties, for example, antistatic characteristics, coloration, stabilisation, reinforcement, UV-resistance, plasticity and flame retardancy. Conventional polymers, including polyethylene (PE), polypropylene (PP), and polyvinyl chloride (PVC) are highly persistent in the environment due to the chemical stability of their polymer backbones. Plastics made from these polymers can fragment into MPs, which may accumulate in soils, are taken up by organisms, or are transported to adjacent ecosystems [6], posing potential environmental risks [24]. Plastics typically have a lower density than natural inorganic sediments such as quartz, clays, silts, and sands. As a result, they tend to stay near the surface in various environments, making them more susceptible to movement. Their behaviour is further influenced by factors like particle size, shape, and surface chemistry, which affect how they interact and aggregate with their surroundings [24].

MPs are defined as particles smaller than 5 millimetres (mm). When larger plastic particles degrade in the environment and fragment into MPs, they are referred to as secondary MPs. They differ from primary MPs, which are intentionally manufactured to be this small from the outset [25]. Primary MPs can be found for example in personal care items, such as exfoliants in cosmetics, where microbeads are incorporated into products like facial scrubs, toothpaste, and shower gels [26], [27]. They are commonly manufactured in the form of pellets, also known as granulates, which typically range in size from 4 mm to 8 mm and are produced in a variety of shapes. The pellets can be made from a wide range of plastic polymers, including PE, PP, polyethylene

terephthalate (PET), polystyrene (PS), and other common plastic types [28]. Additional examples of consumer products other than cosmetics as a source of primary MPs that can be released into the environment include cleaning agents and paints [29].

A general distinction can be made between conventional non-biodegradable plastics and biodegradable polymers (cf. Fig. 1). Hofmann et al. highlighted the key differences and their main characteristics: “In contrast to conventional plastics, biodegradable polymers are designed to undergo microbial metabolic utilization, a process in which the polymer carbon is converted to CO_2 and microbial biomass under oxic conditions. The biodegradability of a polymer depends not only on its physicochemical properties but also on the environmental conditions in which the polymer degrades. Although biodegradable polymers are designed to be ultimately completely mineralized to CO_2, the process may also entail the transient formation of ever-smaller MNP fragments. Biodegradable (and conventional) polymers can be from non-renewable petrochemical or renewable bio-based sources. For example, PBAT is produced from petrochemical sources, while starch, cellulose, chitosan, and PLA are derived from renewable sources” [6].

Building on these observations, the faster degradation rates of certain biodegradable polymers, such as PLA (CAS 9002-97-5) and PBAT (CAS 60961-73-1), compared to conventional plastics like PE, PP and PET (among others), have heightened their appeal in addressing environmental concerns. This interest is driven by their potential to meet essential environmental life cycle requirements [15].

2.1.1 Polylactic Acid and Polybutylene Adipate-co-Terephthalate

One of the most prominent examples of biodegradable polymers is PLA. This aliphatic linear thermoplastic biodegradable polymer can be made from corn, sugar beets, rice and sweet potato, among other fully renewable sources [30]. It features advantages like low energy consumption and low emission of greenhouse gases during production [30]. This biodegradable polymer is used in industrial packaging as well as in the

biocompatible and bioabsorbable medical device market, including applications such as drug delivery systems, implants, sutures and tissue engineering [31]. The production of PLA begins with lactic acid, derived from the bacterial fermentation of sugars [32]. Lactic acid is then converted into a cyclic lactide monomer [33]. During the polycondensation process, water must be removed to prevent the limitation of polymer chain length and to produce high molecular weight PLA [34]. Once the lactide dimer is formed and water is removed, it can be polymerised into PLA without further water generation [33] (Fig. 2).

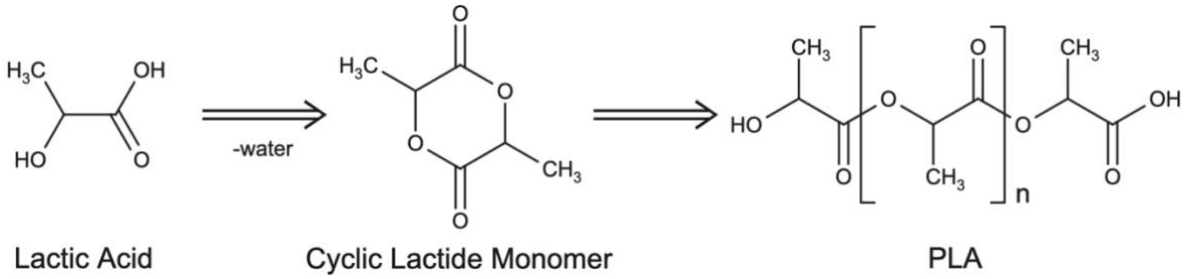

Figure 2: Chemical structure and process of conversion of lactic acid to polylactic acid. Created with Marvin (https://chemaxon.com).

Poly-L-lactide (PLLA), made entirely from the L-isomer of lactic acid, is the most widely used form of PLA (up to 90% of the total PLA market). PLLA has a crystallinity of approximately 37%, which contributes to its structural integrity and performance in various applications. The polymer's glass transition temperature is between 60 °C and 65 °C, while its melting temperature is between 173 °C and 178 °C, indicating its thermal stability. The tensile modulus of PLLA, which measures its resistance to deformation under applied stress, ranges from 2.7 GPa to 16 GPa [35]. This wide range reflects PLLA's ability to provide both stiffness and flexibility, making it suitable for a variety of end-use applications. In addition, PLLA's mechanical strength, thermal resistance and biodegradability contribute to its attractiveness as a sustainable material. However, the high production costs and inherent brittleness of PLA remain significant challenges, limiting its wider commercialisation and application potential [36].

Another extensively used biodegradable plastic, alongside PLA, is the petroleum-based synthetic polyester PBAT, even though recent work investigates the production of PBAT from renewable resources [37], [38]. Owing to its beneficial properties such as low cost, lightweight, and durability, PBAT has become one of the most popular plastics in everyday applications, including food packaging, agriculture (e.g. mulch films), textiles, and other industries. In 2022, the global production of plastics reached 400.3 million metric tons [2], with the aliphatic-aromatic copolyester [39] PBAT accounting for approximately 440 thousand metric tons [40].

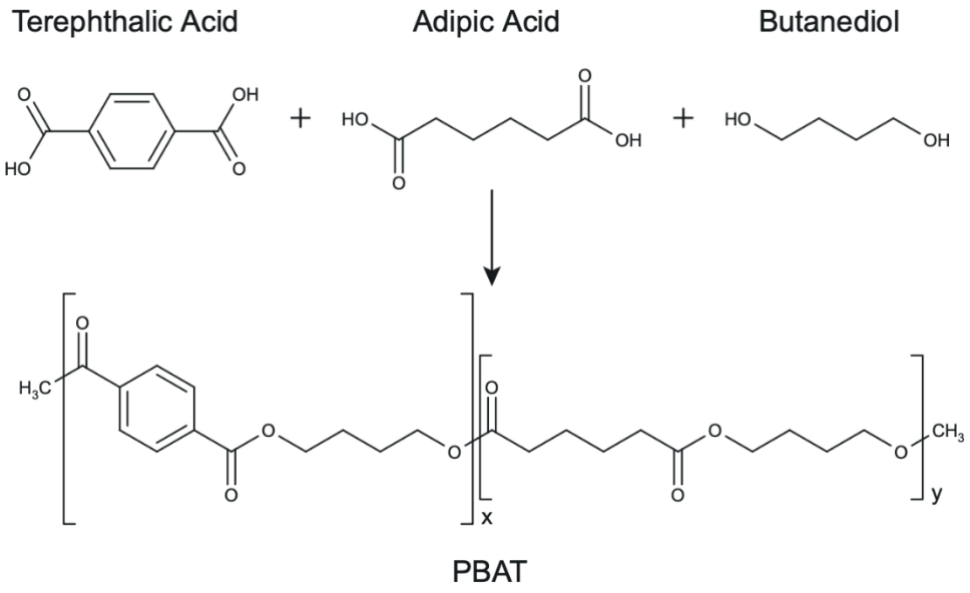

Figure 3: Chemical structure and synthesis of PBAT. Created with Marvin (https://chemaxon.com).

The synthesis of PBAT is achieved through a polycondensation process. Initially, 1,4-butanediol (BDO) undergoes esterification with terephthalic acid (TPA) or transesterification with dimethyl terephthalate (DMT). Next, adipic acid is introduced and reacts with BDO and the terephthalic acid-based oligomers, which leads to the formation of PBAT (Fig. 3) [39], [41], [42].

In addition to the previously mentioned advantages, PBAT is highly flexible due to its butylene adipate segments and offers excellent impact strength and melt processability [41].

2.1.2 Biodegradability

Plastic degradation mechanisms, whether biochemical, photochemical, thermal, or mechanical, are primarily dictated by the polymer's chemical structure. Factors such as the polymer's crystalline and amorphous regions, as well as physical properties like elongation at break (resistance to cracking) and glass transition temperature (the temperature below which plastics become brittle), play a critical role in determining the material's durability and rate of degradation. Additives, while part of the plastic material, are separate from the polymer's intrinsic properties and can influence degradation rates, affecting performance and longevity [24].

PBAT is biodegradable across various environments, including soil and marine ecosystems, owing to its aliphatic segments (butylene adipate), which enhance microbial degradation [42]. This process occurs through both biotic and abiotic mechanisms, although the natural degradation rate of PBAT remains relatively slow [39]. Abiotic degradation mechanisms, such as hydrolysis, photochemical transformation, and thermochemical degradation, primarily target the high-energy chemical bonds in PBAT, resulting in the shortening of polymer chains and a reduction in molecular weight [43]. Recent research by Yang et al. offers a foundation for advancements in enzyme engineering, potentially enabling more effective waste management strategies through enzyme-mediated PBAT biodegradation [39].

PLA primarily degrades via hydrolysis of its ester linkages, with the degradation rate increasing in the presence of higher temperatures and moisture [44]. The breakdown products of PLA include lactic acid, short-chain oligomers, and eventually carbon dioxide and water [45]. While abiotic factors are crucial, microbial activity can also facilitate PLA degradation, particularly in composting environments [46].

Studies on the degradation rates of PBAT and PLA under industrial composting conditions have reported varying results, though it is generally observed that higher temperatures accelerate the degradation process [47], [48]. In a soil microcosm experiment, PBAT exhibited a slightly faster degradation rate than PLA at both 25 °C and 58 °C, with 9.2% of PBAT and 6.1% of PLA degrading after 33 weeks at 58 °C [47]. These

results indicate that under natural conditions, PBAT typically undergoes faster degradation than PLA, although both degrade at relatively slow rates.

2.2 Compost

2.2.1 Production and Use of Compost

Compost is partially decomposed organic material produced through the aerobic, thermophilic breakdown of plant or animal matter by microorganisms [49]. Composting refers to the biological process behind this transformation. The conversion of organic waste into a homogeneous, plant-available material occurs in the presence of oxygen, with adequate moisture and temperature. The sum of complex metabolic processes catalysed by various microorganisms can be defined as composting [50]. The microorganisms involved, particularly bacteria, fungi, and protozoa, act under aerobic conditions with varying intensity depending on factors such as temperature, moisture content, the carbon-to-nitrogen ratio, and the type of organic source material [51]. The microorganisms use the available nitrogen and carbon to produce their biomass. During this process, the microorganisms generate compost with a lower carbon and nitrogen content but higher stability [50]. The composting process can be divided into two main phases: the decomposition phase and the humification phase. The first phase is characterised by microbial activity, during which most of the biodegradable material is broken down, and the organic residue is stabilised. The second phase involves the conversion of part of the remaining organic material into humic substances [52] (Fig. 4). In this way, the composting process resembles the natural processes of mineralisation and humification that occur after the incorporation of organic residues into cultivated soils [53].

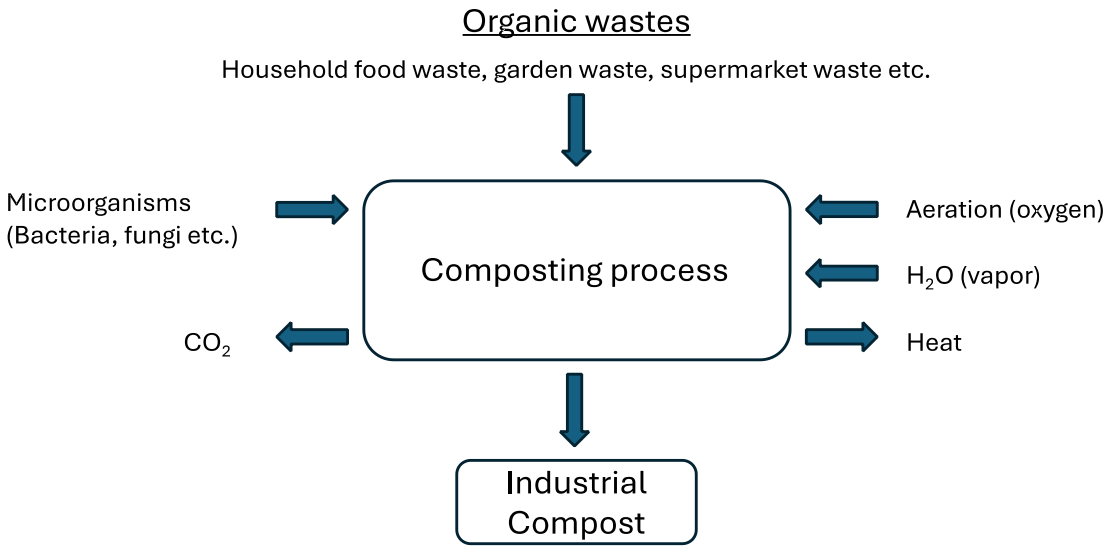

Figure 4: Overview of the composting process with typical organic waste sources in Europe.

Compost is vital to agriculture farmland, improving soil quality and supplying organic matter and nutrients [54]. Composting is an environmentally friendly method for upcycling organic municipal waste, producing a valuable product while reducing waste volume [55]. While garden waste is commonly composted, materials like manure, meat, dairy waste, wood, sawdust, crop residue, and even animal carcasses can also be composted, offering environmental benefits such as reducing groundwater contamination [54]. However, the inclusion of meat and animal-derived waste presents potential hygiene risks, including the spread of pathogens and illnesses, necessitating stringent management practices to ensure safety and prevent contamination. These risks are mitigated through practices such as pasteurisation and high-temperature industrial composting processes among others [56].

Beyond common organic inputs like garden waste or household food waste, other waste streams, such as sewage sludge, are also utilised in compost production. Germany generated nearly 1.8 million metric tons (dry matter) of sewage sludge in 2021, of which approximately 227 thousand tons were recycled for agricultural use, 18 thousand tons for landscaping, and 91 thousand tons for other material recycling, including composting [57]. The European Commission (EC) is currently revising the 1986 Sewage Sludge Directive to address its limited scope, which primarily focuses on heavy metals

and lacks regulations for other significant contaminants, including MPs, pharmaceuticals, and various organic pollutants. Several regulatory options are under consideration, ranging from stricter contaminant limits to a potential ban on the agricultural use of sewage sludge [58]. Consequently, compost is likely to play an increasingly important role in agricultural usage in the coming years.

2.2.2 Regulations in Austria and Germany

Both Germany and Austria, as members of the European Union, must comply with EU regulations like the EU Waste Framework Directive. Each country implements these directives through its national laws. In Austria, this is the Abfallwirtschaftsgesetz (AWG) or "Waste Management Act", and in Germany, the Kreislaufwirtschaftsgesetz (KrWG) or "Circular Economy Act". In alignment with the EU Waste Framework Directive, Section 11(1) of the 2012 KrWg mandates that, starting from January 1, 2015, waste producers and licensed waste management companies must separately collect biowaste. The KrWG places a strong emphasis on the circular economy, prioritising resource efficiency, recycling, and the reuse of materials. Under Section 3 of the KrWG, "biowaste" includes materials from garden, park, and landscape maintenance, as well as food and kitchen waste. This obligation is further clarified by the Biowaste Ordinance (BioAbfV). This ordinance sets clear quality standards for compost and regulates its application to prevent environmental harm.

Similar to Germany, the Austrian AWG requires a separate collection of organic waste. Its focus lies on waste prevention, resource conservation, and environmental protection. Austria has additional guidelines under the Compost Ordinance (Kompostverordnung), which specifically regulates compost quality and usage in agriculture and landscaping.

The standards for composting in both countries include testing requirements for pollutants, organic content and pathogen control. Germany also promotes the use of certified compost, and the Bundesgütegemeinschaft Kompost (BGK) is responsible for overseeing the quality certification of compost. Austria has a decentralised composting

system, which is more regionally controlled through local governments under the AWG, with a stronger focus on compost's use in agriculture. In Germany, the enforcement of the KrWG is carried out at the federal level, with regional authorities responsible for ensuring compliance.

2.2.3 Plastic Found in Compost

Municipal solid waste compost could contain plastic particles, with reported concentrations varying widely. In urban composts, MPs consist mainly of PET, PS, PE and PP, with the highest concentrations found in the 0.63 mm to 1.25 mm size range [59]. Studies have found plastic levels ranging from 0.012-0.046 particles/g [60] to 10-30 particles/g of dry compost [61]. The first study reports particles from 1 micrometre (µm) to 5 mm using light microscopy, which relies on particle colour, shape, and elasticity for analysis. This method is less precise compared to techniques such as Raman Spectroscopy or Fourier Transform Infrared Spectroscopy (FTIR), which offer more accurate particle identification and characterisation. The second study includes data on larger particles, some exceeding 5 mm. The limit for small particles in their study is 25 µm. MP-specific concentrations are reported at 0.007 ± 0.002 particles/g [62] and 5-20 particles/g of dry weight [61]. Additionally, macro- and mesoplastic concentrations of 6.5 g/kg have been reported [62], though direct comparison with particle counts is challenging due to differences in measurement units and measured size ranges. At typical compost application rates in agricultural soils, this could result in the annual introduction of 84.000 to 1.610.000 plastic particles/ha (10.000 m^2) [60] or higher [62]. These reported values span a broad range, from as low as 0.012 particles/g [60] to as high as 30 particles/g of dry compost [61]. However, particle numbers are not a meaningful measure to elucidate whether these numbers are of concern, or not. Beside particle number, particle size, size distribution, mass and polymer composition, the analysis should include possible intentionally used additives or adsorbed substances.

2.3 Extraction Methodologies of Plastics

Although density separation is a common method for characterising MPs in aquatic sediments [63], it is less effective for soil, compost and sludge samples due to the high content of organic matter and the presence of complex organic compounds [21]. Soil organic matter and certain MPs, such as PET, share comparable densities (1.0 – 1.4 g/cm^3), complicating their separation [64]. Similar challenges are encountered in compost samples. Consequently, additional pretreatment steps are necessary to remove organic matter without degrading the MPs, ensuring accurate analysis.

Polymer-mass-based techniques for extracting MPs from soil samples, such as pressurised liquid extraction, thermal decomposition coupled with gas chromatography-mass spectrometry (GC-MS), and rapid heat pretreatment, are designed to dissolve or pyrolyze MPs rather than preserve their physical structure. These methods eliminate the need for sample pretreatment and focus solely on determining polymer concentrations [21]. However, they do not allow for the analysis of particle size, shape, or surface properties, which are critical for understanding the environmental behaviour and ecotoxicological impacts of MPs. In contrast, non-destructive methods can enable the visualisation of particles and provide data on their size, shape and distribution.

To enable and improve the non-destructive extraction of MPs from organic-rich matrices as e.g. compost, it is vital to reduce the concentration of natural organic matter in the samples. To effectively remove organic matter in complex, organic-rich environmental matrices, various techniques have been explored, including hydrogen peroxide (H_2O_2), Fenton's reagent, alkaline digestion, and sodium hypochlorite (NaOCl) [21], [65], [66], [67]. Fenton's reagent has shown the most promising results for sewage sludge samples, offering rapid and efficient organic matter removal with minimal impact on most polymers [21], [65]. In freshwater samples, a 7% NaOCl solution has demonstrated high organic matter removal and high polymer recovery rates [66]. NaOCl treatment can also enhance MP detection in soil organic matter, though recovery rates vary depending on MP size, polymer type, extraction method, and soil type [68]. Based

on these findings, this work focuses on optimising Fenton's reagent for a more efficient, cost-effective approach for organic matter removal before MP extraction.

2.4 Fenton Reaction

The Fenton reaction, first described by Henry J. Fenton in 1894, involves the activation of H_2O_2 by iron (Fe) ions, producing highly reactive hydroxyl radicals (OH•). They are strong oxidising agents capable of breaking down a wide variety of organic and inorganic substances. Over the past century, Fenton chemistry has attracted considerable interest due to its relevance in biological processes, environmental remediation and industrial applications. The reaction mechanism, later refined by Haber and Weiss in 1934 and further elaborated by Barb et al. in the mid-20th century, is now known as the commonly accepted process and generally referred to as the Fenton chain reaction with the production of OH• radicals as the key step [69].

The Fenton chain reaction can be outlined in the following four steps, forming a continuous cycle:

(1) $Fe(II) + H_2O_2 \rightarrow Fe(III) + OH\bullet + OH^-$

(2) $Fe(III) + H_2O_2 \rightarrow Fe(III)(O_2H^-) + H^+$

(3) $Fe(III)(O_2H^-) \rightarrow HO_2\bullet + Fe(II)$

(4) $Fe(III) + HO_2\bullet \rightarrow Fe(II) + O_2 + H^+$

Ferrous iron (Fe^{2+}) reacts with hydrogen peroxide (H_2O_2) to produce ferric iron (Fe^{3+}), a hydroxyl radical (OH•), and a hydroxide ion (OH^-) (1). The Fe^{3+} formed in this reaction can then react with another molecule of H_2O_2, resulting in the formation of the complex Fe(III)(O_2H^-) and a proton (H^+) (2). This step is referred to as the "Fenton-like" reaction

[70]. The Fe(III)(O_2H^-) complex subsequently decomposes, generating a hydroperoxyl radical (HO_2•) and regenerating Fe^{2+}, which enables the continuation of the Fenton reaction (3). Additionally, Fe^{3+} reacts with the HO_2• radical, producing oxygen (O_2), releasing a proton (H^+), and regenerating Fe^{2+} (4). This cyclic process ensures the continuous generation of OH• radicals, driving the reaction forward. The Fenton reaction can continue as long as there is a supply of reactants. The oxygen produced in step (4) typically escapes as a gas (depending on the environment and reaction setup). The protons produced in steps (2) and (4) remain in the solution, increasing the acidity as the reaction progresses. This can affect the reaction rate and overall efficiency of the Fenton process, as the optimal pH for oxidative degradation of organic contaminants is slightly below 3 [69].

Although Fenton has proven successful as a pretreatment method for extracting MPs from organic-rich matrices, significant variability in techniques and applications complicates comparisons between studies. Therefore, it is important to develop a standardised method for applying Fenton in the pretreatment process to ensure consistency and comparability.

2.5 Microplastics Analysis Techniques

The analytical observation techniques for MPs can be broadly categorised into two main methodologies: counting/particle-number-based and bulk/particle mass-based.

The first group focuses on identifying and counting individual MP particles, often using microscopy and spectroscopy techniques such as Optical Microscopy, Electron Microscopy (SEM/TEM), FTIR and Raman Spectroscopy. Optical Microscopy, usually coupled with fluorescence, is the most common technique used for identifying MP. Particles are counted and characterised based on size, shape and colour. However, it cannot chemically identify the plastics, is labour-intensive and susceptible to human error [71]. Scanning Electron Microscopy (SEM) and Transmission Electron Microscopy (TEM) can reveal detailed surface characteristics and microstructures [72] but are time-consuming and cannot distinguish plastic from natural organic matter. FTIR and μ-FTIR

are widely used for determining the chemical composition of MPs [73], [74]. This is done by analysing the absorption of infrared light, allowing for identification by comparing spectra with reference materials. Similarly, Raman spectroscopy identifies the chemical composition of MPs [73] by measuring molecular vibrational modes [75].

The second group (bulk/particle mass-based methods) measure the total mass of MPs in a sample rather than counting individual particles. They are useful to understand the overall burden of MPs in each environment. Nuclear Magnetic Resonance Spectroscopy (NMR) analyses the magnetic properties of nuclei in a polymer chain and provides information on the chemical structure and the concentration (quantitative NMR) of MPs in a sample [76]. Pyrolysis-gas chromatography-mass Spectroscopy (Pyrolysis GC-MS) is frequently used to identify polymer types and quantify the mass of MPs in environmental samples. Pyrolysis GC-MS heats the MP sample to break it down into smaller molecules (pyrolysis), which are then separated by gas chromatography and identified by mass spectrometry [77].

3 Aims & Hypotheses

In the current understanding of plastics, significant knowledge gaps remain regarding the behaviour of both persistent and degradable MPs in compost. These gaps are primarily due to challenges in extracting and analysing MPs from such complex organic matrices. Existing methods, while generally more effective for persistent plastics, often rely on harsh conditions that risk damaging or altering biodegradable plastics such as PLA and PBAT. Moreover, these methods can be time-consuming and resource-intensive. A further complication is the lack of standardised protocols for applying Fenton oxidation, which shows promise but exhibits inconsistent results across studies. Developing gentle yet effective extraction methodologies is essential to enable accurate analysis of biodegradable plastics, improve our understanding of their persistence in compost, and assess their potential long-term impacts as contaminants.

Pfohl et al. examined the effects of the Fenton reaction on the polymer structure of PLA and PBAT, among other materials. They compared the surface textures, chemical composition, and particle size distributions before and after digestion. Their findings indicated that the Fenton protocol left the surfaces of the biodegradable polymers largely unchanged [78]. However, the oxidation process did lead to a reduction in particle sizes and alterations in particle size distribution. Wohlleben et al., using the same protocol, showed that the particle size distribution of the investigated aromatic-aliphatic polyester (PLA-based) was not affected [79].

The primary objectives of this study are to optimise the Fenton reagent method, balancing effective organic matter removal with minimal impact on degradable plastics (specifically targeting improvements in time efficiency, cost reduction, separation quality, and plastic recovery), and to evaluate the effect of this method on degradable plastics. To achieve these objectives, two main hypotheses have been formulated:

Hypothesis 1

Variations in the concentrations of hydrogen peroxide and iron catalysts will allow for finding an optimal condition that maximises organic matter removal from compost. These conditions provide MP integrity, though optimal conditions may not align with complete organic matter removal.

To test this hypothesis, homogenised, native compost is subjected to various organic matrix removal procedures adapted from previously published protocols [21], [68], [78], [79]. The effectiveness of these procedures is evaluated by comparing weight differences and total organic carbon content before and after treatment.

Hypothesis 2

Under previously optimised conditions, the integrity of degradable polymers is maintained during organic matter removal. Given the low temperature and controlled parameters, the degradable plastics should not suffer significant damage.

To verify this hypothesis, PLA and PBAT are subjected to the most promising organic matrix removal procedure from hypothesis 1. They are then analysed using digital optical microscopy, open-source image processing software Fiji [80], and statistical evaluation in RStudio [81].

4 Materials & Methods

This section provides an overview of the methods used to enhance organic matrix removal in compost samples without the use of harsh conditions. Fenton oxidation and NaOCl are tested as an oxidation agent for organic matter removal. To determine the most efficient mixture of hydrogen peroxide and iron catalyst ($FeSO_4$) concentrations, a total of 19 different Fenton procedures were performed (Tab. 1). In addition, two NaOCl oxidations with different concentrations were carried out. Each procedure was performed in triplicate, except the NaOCl and (Fenton) ultrasonic treatments. Following the Fenton treatments, samples were filtered to collect the solid residue and weight loss was measured as an initial estimate of organic matter removal. For a more accurate quantification of organic matter removal, the most promising samples were analysed using a multiphase carbon and water analyser (LECO RC612). After determining the optimal concentrations of the reagents, polymers were subjected to the same treatment in the absence of compost and then examined using digital optical microscopy. Next, the polymers were analysed for particle size (mean area) and distribution using Fiji [80], and the data were statistically examined with RStudio [81]. Detailed descriptions of sample preparation and measurement procedures are provided below.

4.1 Organic Matrix Removal

4.1.1 Organic Matrix Removal by Fenton Oxidation

A stock solution of iron (II) sulphate heptahydrate was prepared (7.5 g $FeSO_4$ x 7 H2O in 500 mL Milli-Q water), and the pH of the solution was adjusted to a value between 3 and 4 using a 2 M solution of hydrochloric acid (HCl). Acidic conditions help to prevent the precipitation of insoluble iron species, preserving the catalytic activity of Fe^{2+} and, therefore, the generation of hydroxyl radicals [82]. Compost is previously sieved through

a 1 mm sieve, and any aggregates in it are broken up, achieving a homogenised solid sample. First, one gram of native compost was weighed in a beaker and filled with 40 mL of Milli-Q water (Milli-Q). The compost-Milli-Q mixture was then treated with ultrasound (Bandelin Sonopuls, big tip) for five minutes at 40 watts. Three samples were placed on magnetic stirrers. The pH values were measured again and, if necessary, adjusted to the target value between 3 and 4 with additional HCl. Temperature was measured continuously during the experiment. The experiments were performed with different amounts of H_2O_2 (35%) as an oxidant and ferrous sulfate ($FeSO_4$) solution as a catalyst. Different addition variants were tested: direct addition, dropwise addition, and direct addition in an ultrasound bath (Fig. 5, a-c).

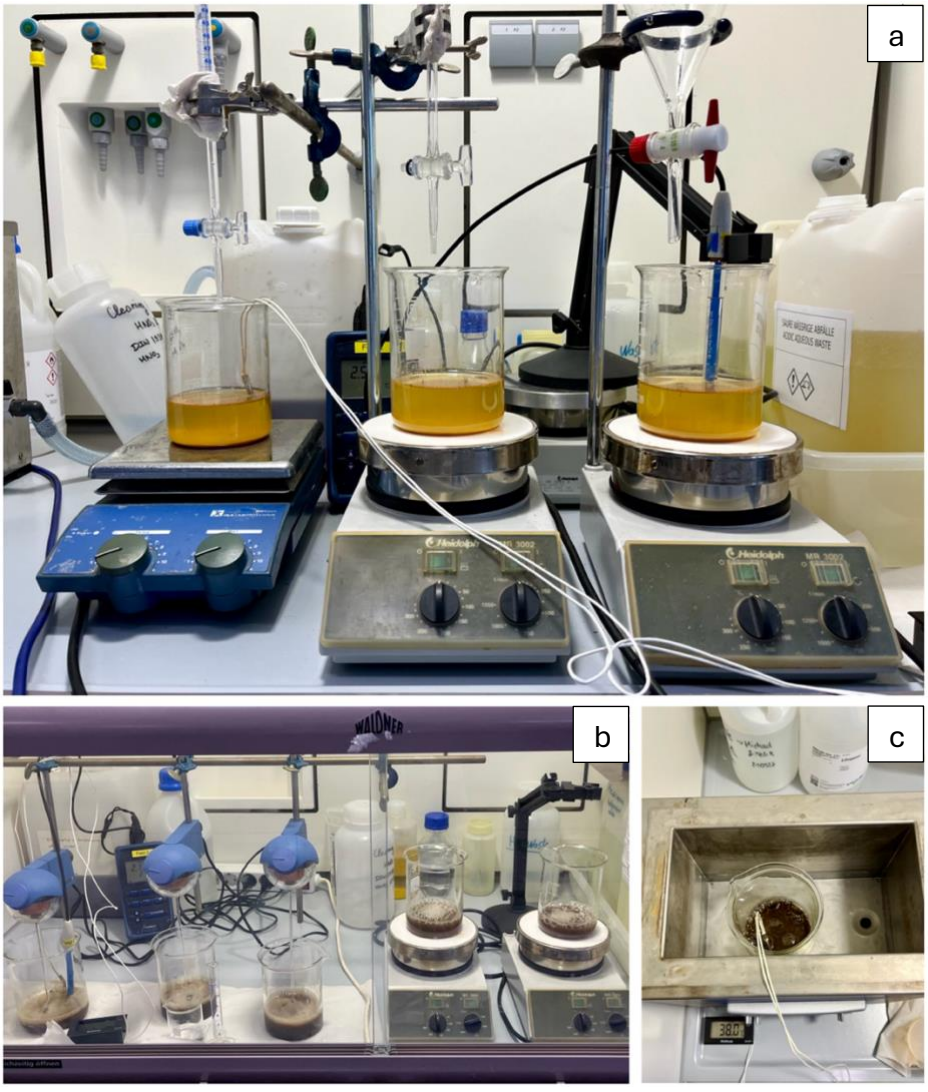

Figure 5: Overview of various Fenton oxidation procedures. a: Dropwise addition, b: General procedure with direct addition, c: Fenton oxidation in an ultrasound bath.

The most frequently applied standard procedure comprised five direct additions of varying volumes of H_2O_2 and $FeSO_4$ solution every 30 minutes (Tab. 1). After the last addition, the Fenton compost mixture was stirred for a further 30 minutes and then left to rest for 60-90 minutes to finish the reaction and allow the remaining particles to settle to the bottom of the beaker. The temperature and pH values were measured before the first addition and during the whole duration of the oxidation experiment. The samples were then vacuum filtered over glass microfibre filters (VWR type: 692, size: 47 mm, particle retention: 1.0 µm) to obtain the solid compost residue (Fig. 6e).

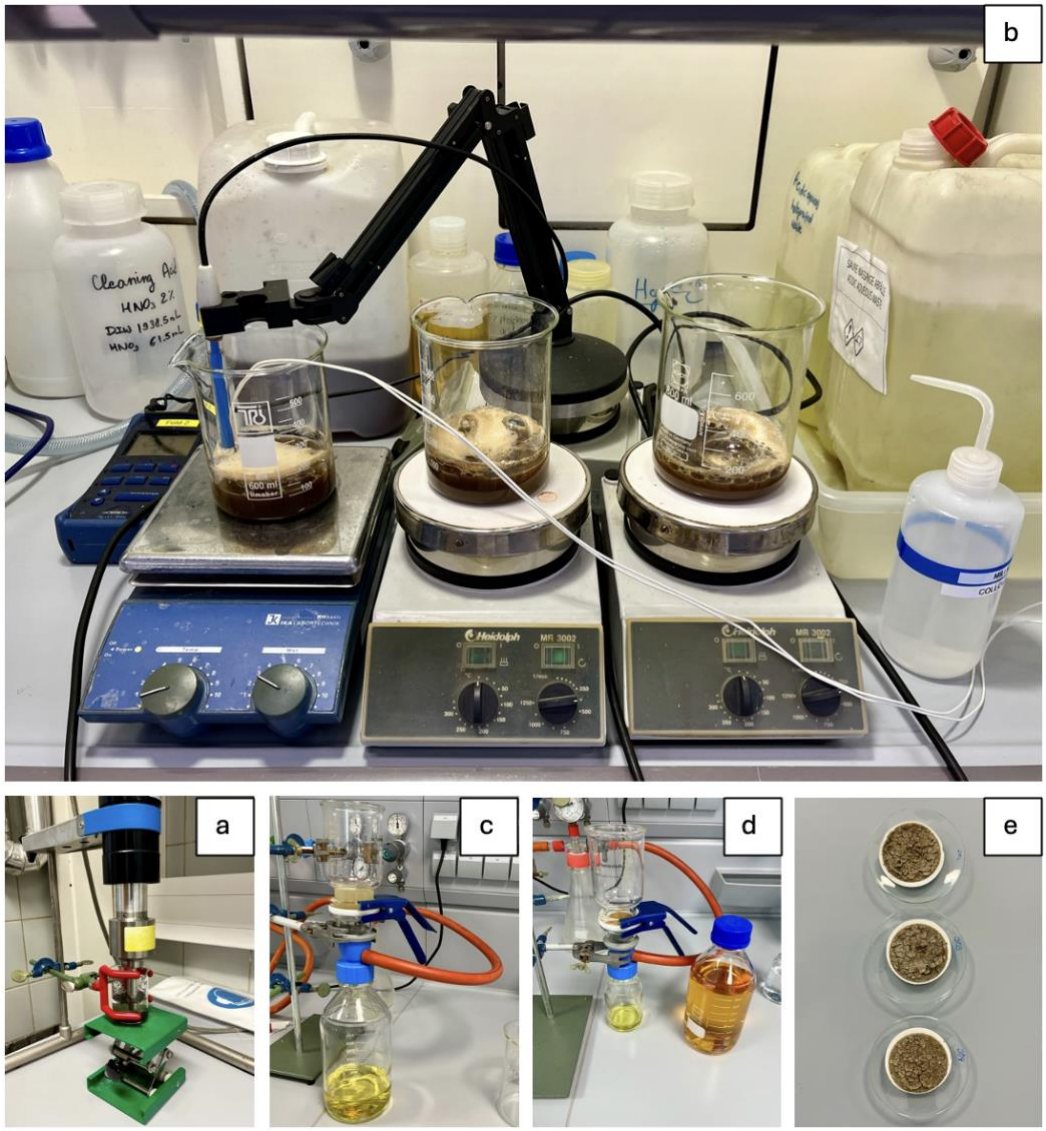

Figure 6: The images illustrate the general Fenton oxidation and filter procedure. They demonstrate the following stages: sonication of the compost sample in Milli-Q (a), samples during Fenton oxidation (b), filtering of the Fenton-compost solution (c), addition of HCl onto filters after filtering the Fenton-compost solution (d), and the solid compost residue after drying (e).

Table 1: Overview of the tested organic matrix removal protocols, summarising the various reagent concentrations and the key procedural conditions (see Chapter 4.1 for details). For $FeSO_4$, 0.05 M corresponds to approximately 15 mg/mL and 0.07 M to 20 mg/mL.

Reagents Concentration	Procedure Conditions
5 x 15 mL H_2O_2 (35%), 5 x 10 mL $FeSO_4$ (0.05 M)	30 minutes in between doses, direct addition
5 x 15 mL H_2O_2 (35%), 1 x 20 mL $FeSO_4$ (0.05 M)	30 minutes in between doses, direct addition
5 x 10 mL H_2O_2 (35%), 5 x 10 mL $FeSO_4$ (0.05 M)	30 minutes in between doses, direct addition
5 x 15 mL H_2O_2 (35%), 5 x 10 mL $FeSO_4$ (0.05 M)	30 minutes in between doses, direct addition
5 x 25 mL H_2O_2 (35%), 5 x 10 mL $FeSO_4$ (0.05 M)	30 minutes in between doses (5 mL H_2O_2 every 5 minutes), direct addition
5 x 25 mL H_2O_2 (35%), 5 x 25 mL $FeSO_4$ (0.05 M)	30 minutes in between doses, direct addition, heated to 50 °C, maximum removal test
5 x 5 mL H_2O_2 (35%), 5 x 5 mL $FeSO_4$ (0.05 M)	30 minutes in between doses, direct addition
5 x 25 mL H_2O_2 (35%), 5 x 25 mL $FeSO_4$ (0.05 M)	30 minutes in between doses, direct addition, maximum removal test
5 x 15 mL H_2O_2 (35%), 1 x 25 mL $FeSO_4$ (0.05 M)	30 minutes in between doses (10 mL H_2O_2 every 10 minutes), direct addition
5 x 10 mL H_2O_2 (35%), 5 x 5 mL $FeSO_4$ (0.05 M)	30 minutes in between doses, direct addition
75 mL H_2O_2 (35%), 1 x 30 mL $FeSO_4$ (0.07 M)	Dropwise addition of H_2O_2 (time independent), direct addition of $FeSO_4$ at start
5 x 10 mL H_2O_2 (35%), 5 x 5 mL $FeSO_4$ (0.07 M)	Dropwise addition of H_2O_2, $FeSO_4$ every 30 minutes, 5 mL HCl 2M onto filters
5 x 20 mL H_2O_2 (35%), 5 x 10 mL $FeSO_4$ (0.07 M)	Dropwise addition of H_2O_2, $FeSO_4$ every 30 minutes, 5 mL HCl 2M onto filters
5 x 10 mL H_2O_2 (35%), 5 x 10 mL $FeSO_4$ (0.07 M)	Dropwise addition of H_2O_2, $FeSO_4$ every 30 minutes, 5 mL HCl 2M onto filters
5 x 10 mL H_2O_2 (35%), 5 x 10 mL $FeSO_4$ (0.07 M)	30 minutes in between doses, direct addition, 5 mL HCl 2M onto filters
5 x 10 mL H_2O_2 (35%), 5 x10 mL $FeSO_4$ (0.07 M)	30 minutes in between doses, direct addition, ultrasound bath, 5 mL HCl 2M
5 x 25 mL H_2O_2 (35%), 5 x 25 mL $FeSO_4$ (0.07 M)	30 minutes in between doses, direct addition, 5 mL HCl 2M onto filters, maximum removal test
Wohlleben et al. (2023) protocol	Performed over 2 days, 2 hours in between doses, 5 mL HCl 2M onto filters
Sodium Hypochlorite	a) 1 M NaOCl, b) 2.023 M NaOCl (both: direct addition, dry compost, 2.5 hours reaction time, compost/solution ratio 1:5)
5 x 10 mL H_2O_2 (35%), 5 x 10 mL $FeSO_4$ (0.05 M)	30 minutes in between doses, direct addition, 5 mL HCl 2M onto filters

After filtration, the filters were dried (60 °C, 16 hours) and weighed to obtain the residual mass of the compost after Fenton treatment. The determined weight loss serves as an approximation of the removal efficiency achieved (Eq. 1). The results of all the procedures described above were then compared, and the most promising samples were analysed for an exact organic carbon value using a multiphase carbon and water analyser (LECO).

Equation 1: Mass removal efficiency (η)

$$\eta = \left(\frac{m_{\text{compost, initial}} - (m_{\text{filter, final}} - m_{\text{filter, initial}})}{m_{\text{compost, initial}}}\right) \times 100\%$$

- $m_{\text{compost, initial}} =$ Mass of the compost before Fenton oxidation
- $m_{\text{filter, initial}} =$ Mass of the filter before filtration
- $m_{\text{filter, final}} =$ Mass of the filter after drying (post-filtration)

4.1.2 Organic Matrix Removal by Sodium Hypochlorite

The NaOCl method was conducted according to Bottone et al. using 1 g of compost as in the Fenton oxidation procedures (see Chapter 4.1.1). The protocol they presented used 1 M NaOCl with a soil/solution ratio of 1:5 [68]. Here, a 10-15% active chlorine solution of NaOCl (Thermo Scientific) was used. Assuming its molarity to be 2 M (12.5% active chlorine; see SI for calculations), it was diluted with Milli-Q to 1 M. At a compost-to-solution ratio of 1:5, the 1 M NaOCl solution was applied directly to the dry, non-ultrasonicated compost. The filtration process and calculation of mass removal efficiency followed the same protocol as the Fenton procedure to ensure comparability. Temperature and pH were measured and recorded every 30 minutes (see SI Tab. S2). An additional NaOCl oxidation was performed using the 2 M NaOCl solution directly.

4.2 Carbon Analysis

A multiphase carbon and water analyser by LECO (RC612) was used to determine the total carbon content (TC), the total inorganic carbon content (TIC), and the total organic carbon content (TOC) of the compost samples before and after the Fenton procedure.

The analysis of TC, TIC and TOC is conducted as follows: The furnace is purged with oxygen to create an oxidising environment that facilitates the combustion of carbon and the evaporation of water (H_2O). To ensure complete combustion or reaction of all released components, the system includes an afterburner furnace, typically set at 850 °C, along with a secondary oxidation catalyst. The resulting combustion products are quantified using infrared detection, and the results are reported as either a weight percentage or a coating weight [mg/in^2]. In an oxidising atmosphere (O_2), most carbon forms are converted to carbon dioxide (CO_2), except for certain carbides, such as silicon carbide (SiC). Organic carbon is distinguished by its combustion products, which include both H_2O and CO_2, allowing for its identification through the detection of simultaneous H_2O and CO_2 peaks [83].

Before use, the instrument must be preheated to 1000 °C, and the calibration curve must be corrected for drift (see SI for details). This is done to ensure the stability and high yield of the catalysers that the instrument uses.

4.2.1 Determination of the Combustible Fraction Using Loss-on-Ignition and Carbon Analyser

The combustible fraction of the native compost samples was determined using loss-on-ignition (LOI) analysis and LECO carbon analyser, employing two different temperature profiles. LOI analysis was conducted at 550 °C for four hours in a high-temperature oven (Nabertherm P 330). Before loading the samples into the high-temperature oven, ceramic vessels were pre-heated to 550 °C to remove any present organic material and moisture (Fig. 7). Then, 1 g of compost was added to each vessel and placed in the same

oven at 550 °C for approximately four hours. After the vessels had cooled down, they were weighed again, and the mass removal was calculated (see SI for details). LECO analysis was performed using a temperature gradient ("Rampe-CA" furnace method: 100 °C to 1000 °C in 32 minutes) in a LECO furnace (RC612).

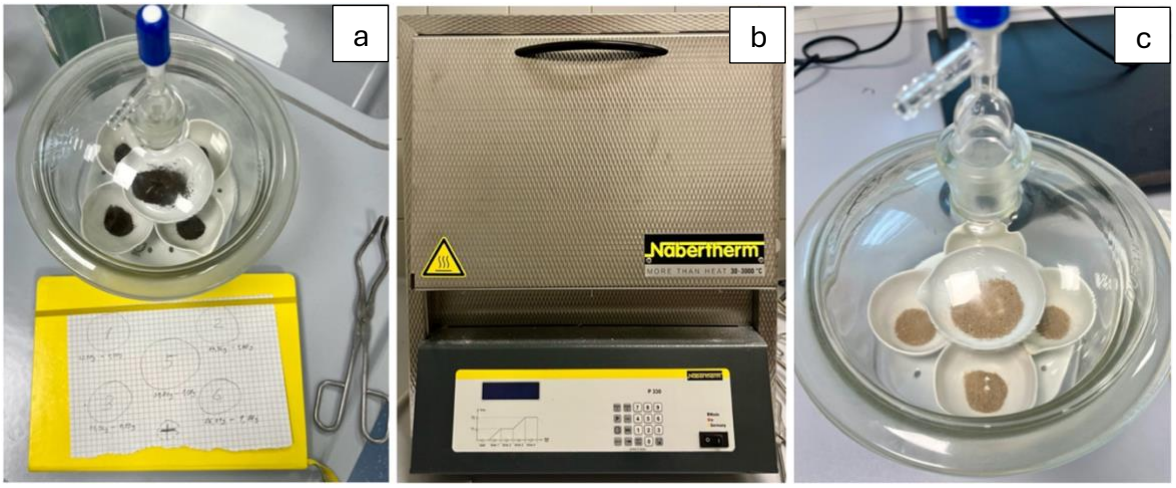

Figure 7: Determination of the combustible fraction of native compost. Native compost in ceramic vessel before combustion (a), high-temperature oven (b), native compost in ceramic vessel after combustion placed in a desiccator (c).

4.2.2 Total Organic Carbon Analysis

After drying the filters in a drying cabinet for approximately 16 hours at 60 °C (as detailed in Chapter 4.1), they were prepared for LECO analysis. Initially, several compost samples that had not undergone the Fenton procedure were analysed to determine an appropriate sample weight that would avoid oversaturation beyond the instrument's saturation limit and to establish a baseline for assessing the removal efficiency of the Fenton method. A slow ramping temperature program was selected, increasing from 100 °C to 1000 °C over approximately 32 minutes, to separately identify the peaks of organic and inorganic carbon. A sample weight of approximately 0.025 g provided optimal results and was used for all subsequent measurements of untreated compost samples. The average value from the measurements of native compost was used for comparison and to calculate the removal efficiency.

An initial attempt was made to quarter the Fenton-treated samples on the filter using a scalpel, weigh the segments, and calculate the compost weight based on the known filter weight. However, the compost weight on the quartered filter was approximately 0.2 g, exceeding the saturation limit of the instrument. Instead, the dried Fenton/compost residue was scraped from the filter into a small glass bowl using a metal spatula, ensuring no filter material was included, which could affect measurement accuracy. The residue was homogenised with a metal spatula to ensure that the scraped material represented the entire sample and to prevent high-intensity peaks caused by, e.g., small wood fragments (Fig. 8a).

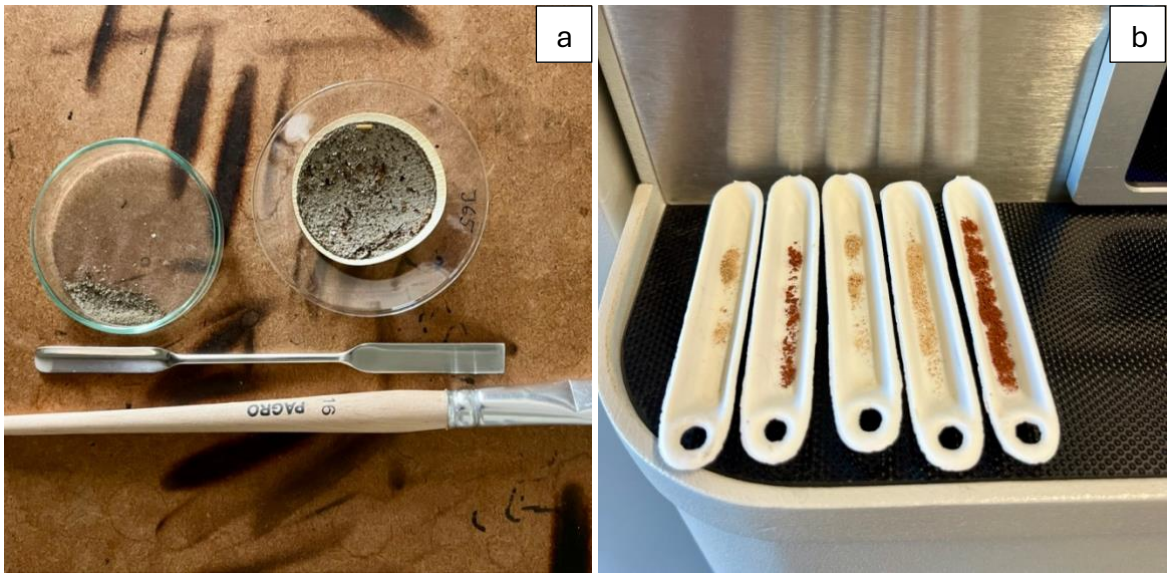

Figure 8: Measurement of TOC values. Fenton/compost residue preparation (a). Samples after combustion and TOC measurement, note: the reddish samples are from the maximum removal tests and clearly show the increased iron content (b).

A limitation of this technique is that the residue mass includes iron precipitated from the Fenton reaction, causing variability in the mass balance depending on the iron content. A visual indication of this is the reddish colour after combustion (Fig. 8b). To address this issue, HCl was added to the filters after filtration to dissolve the iron precipitates, enabling more accurate measurements with the LECO. Because of its strong acidic nature, HCl initiates a dissolution process by providing H^+ ions, which react with the iron precipitates (such as iron oxides or hydroxides), converting them into

soluble Fe^{2+} and Fe^{3+} ions. These ions then form soluble complexes with the chloride ions (Cl^-) from HCl, resulting in iron(II) chloride ($FeCl_2$) and iron(III) chloride ($FeCl_3$). This process effectively removes the iron precipitates from the filters under low pH conditions. Detailed results of individual TOC measurements are provided in the SI.

4.3 Polymer Size and Morphology Analysis

4.3.1 Fenton Oxidation and Filter Process

To evaluate the effects of ultrasonication, the Fenton reaction, and their combined impact on polymer size distribution and morphology, a series of experiments was conducted (Fig. 9).

Initially, two solutions were prepared, each containing 14 mg of polymer particles dispersed in 50 mL of Milli-Q water: one with PBAT particles (100–300 µm) and the other with PLA particles (125-249 µm). Tween 20, a surfactant, was added to prevent particle aggregation. All experiments were performed separately for each polymer.

Control samples representing the untreated state were directly filtered to determine the initial size distribution of the polymer particles. Experimental treatments involved mixing 2 mL of each polymer suspension with 40 mL of Milli-Q water, followed by ultrasonication alone, Fenton oxidation alone, or a combination of both treatments (complete procedure, Fig. 9a) as described in Chapter 4.1. The Fenton oxidation procedure, previously identified as the most effective, based on mass removal efficiency and TOC measurements, was applied in the treatments involving Fenton oxidation.

After treatment, the particles were filtered using PALL Supor 800 filters (0.8 µm, 47 mm). All filters were placed on a flat surface, covered to prevent dust contamination, dried overnight (Fig. 9b-c), and subsequently analysed under a digital optical microscope to assess changes in size distribution and morphology (Fig. 9d).

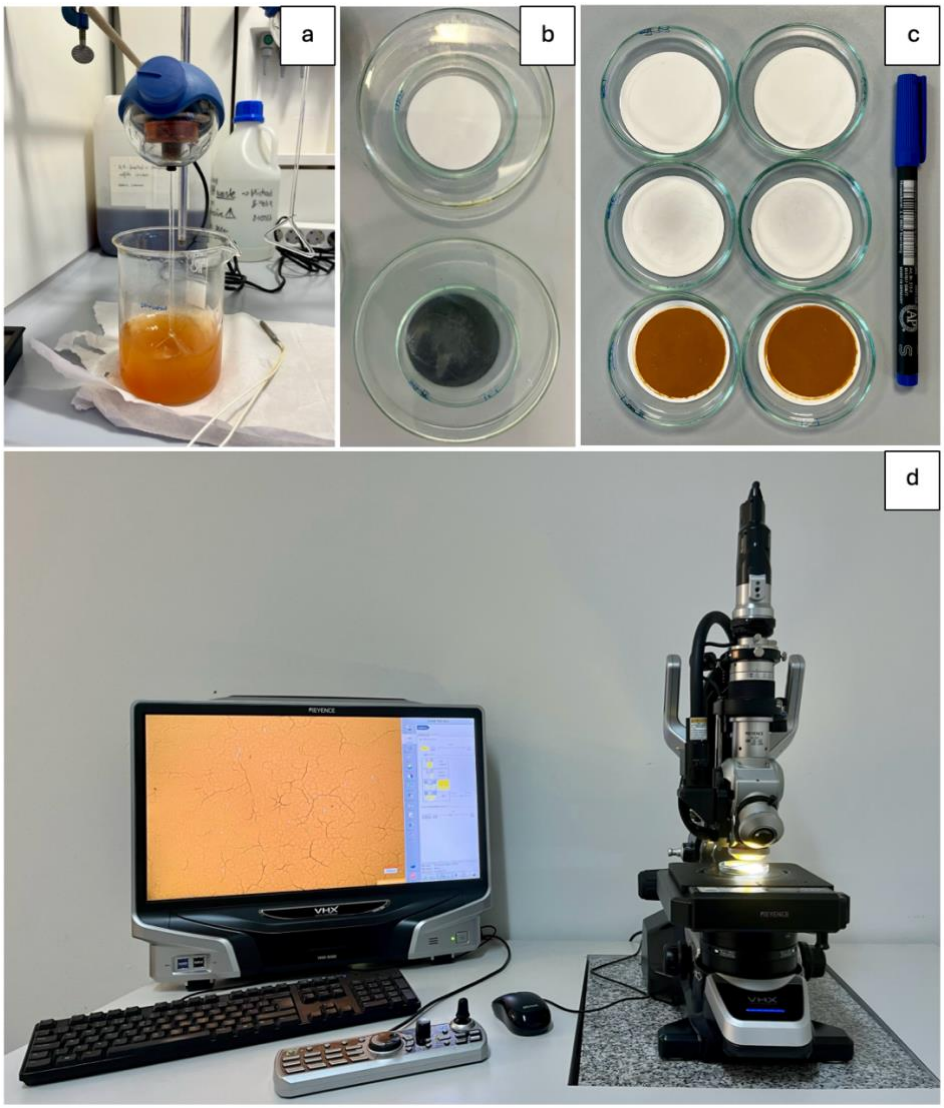

Figure 9: Polymer stability test. Fenton oxidation (a). Testing of different filters (b). Polymer particles on filters in the untreated state, after sonication, after Fenton oxidation (c). Digital optical microscopy of a filter containing particles treated with Fenton, preliminary step for size distribution analysis (d).

4.3.2 Digital Optical Microscopy and Particle Analysis

Using a Keyence digital microscope (VHX-Series 5000), digital images of the polymer particles on the filters were captured and saved at various magnifications (20x, 30x, or 50x). The 2D stitching tool was employed to ensure comprehensive visualisation of all particles on the filter. This also streamlined subsequent analysis with Fiji [80] by allowing more particles to be analysed simultaneously within the same image. The optimal microscope settings for capturing high-quality images were as follows:

- For untreated PBAT and PLA samples: HDR (ClearImage) or High-Resolution HDR with full coaxial lighting.
- For Fenton-treated PBAT and PLA samples: full ring lighting, occasionally using the "Image Quality UP" function for glare removal.

Once optimal lighting conditions were established and it was confirmed that no particles were recorded more than once, the obtained images were analysed using Fiji [80].

The scale within the image was marked using the straight lines tool and calibrated with the "Set Scale" function. To enable automatic particle analysis, the image was converted to a binary (black and white) format by transforming the RGB colour image into an 8-bit type image. A threshold range was set to distinguish all visible particles from the background. Pixels below the threshold were converted to black, and those above the threshold to white, or vice versa. The "Analyze Particles" function was then used to assess the particles in the segmented image, with a minimum particle size set to 2500 μm^2 to ensure that only plastic particles were included.

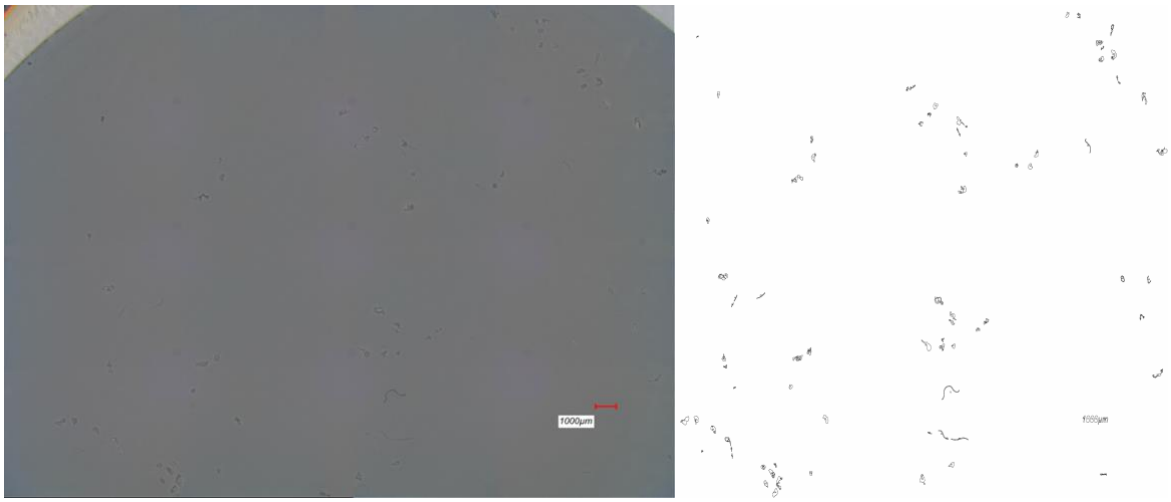

Figure 10: Left: Original microscope image, right: outline drawing of particles created with Fiji [73].

The detected particles were then compared with the original image to confirm that they were indeed plastic particles and not artefacts resulting from lighting issues in the original image editing process (Fig. 10).

After completing particle analysis for all relevant images, statistical analyses were conducted using RStudio [81].

4.4 Statistics

Statistical analysis of organic matrix removal by mass, TOC values, and polymer size distributions—both with and without treatment—was conducted using RStudio [81]. The first step assessed the mass removal efficiency (%) determined by weight differences, as described in Chapter 4.1. The results of the best-performing organic matter removal method of this study were compared with those obtained using the method developed by Wohlleben et al. [79] (hereinafter referred to as the Wohlleben et al. 2023 method). Boxplots were employed to effectively illustrate the distribution, central tendency, and variability of the data, providing a clear visual comparison between the two methods. Next, TOC values obtained via LECO analysis were compared across untreated compost, the best-performing Fenton procedure, and the Wohlleben et al. (2023) method. This comparison aimed to evaluate the extent of organic carbon removal achieved by each method, serving as a key indicator of their effectiveness in degrading organic matter in compost. Additionally, particle size data from individual samples, analysed using Fiji [80], were compared. Descriptive statistics, including count, mean, standard deviation, median, and interquartile range, were calculated to summarise the particle size distribution. Boxplots and histograms were generated to visually assess the shape of the distribution. To test for normality, the Shapiro-Wilk test was performed, as it provides reliable insight into whether the data follows a normal distribution. Since none of the datasets met this assumption, the non-parametric Mann-Whitney U test was applied for inferential statistics to compare the central tendencies between samples and determine if they significantly differ. This test was chosen for its robustness in handling non-normally distributed data. The results

were considered significant at a p-value of 0.05. Additionally, rank-biserial correlation was calculated to measure effect size and assess the strength of association between variables. This non-parametric method helps to understand how strongly changes in one variable are related to changes in another and adds additional insight about statistically significant differences between the analysed samples. Furthermore, polymer size distributions under various conditions (pristine, sonication, Fenton, and complete treatment) were analysed, focusing on the D10, D50 (mean), and D90 values. These percentiles were selected to provide a comprehensive overview of particle size distributions, capturing both smaller and larger particle fractions. This approach offers additional insights, apart from the mean and standard deviation, into how each treatment affects the integrity of the polymers. All R scripts used in these analyses are provided in the SI.

5 Results & Discussion

5.1 Effect of Different Fenton Reagent Conditions on the Degradation Efficiency of Organic Matter in Compost

For the accurate detection and measurement of MPs from the environment, it is important that the laboratory procedure does not alter them. Extraction conditions must preserve plastic particle integrity. Previous studies have demonstrated that elevated temperatures can increase the production of hydroxyl radicals, which would increase the degradation of organic matter [84]. However, this can also impact the stability of biodegradable polymers and their physiochemical properties [47]. Since the glass transition temperature of PLA is approximately 60 °C [35], higher temperatures might cause softening and degradation of the particles. Furthermore, higher temperatures can enhance the hydrolysis of ester bonds in both PLA and PBAT, which in turn increases the degradation rate [47]. Long exposure to oxidative conditions could increase the organic matter degradation but may gradually impact the polymer's stability. The combined effects of hydrolysis and oxidative degradation at elevated temperatures can result in a more extensive and rapid breakdown of the polymers. Moreover, a recent study has demonstrated that conventional plastics, including polystyrene nanoplastics (140 nm), can be completely degraded through Fenton procedures at 80 °C [22]. This involved an initial pH of 3, with 15 doses of hydrogen peroxide (7.5%, 1 mL each) added every 30 minutes and five doses of ferric ion (750 mg/L, 1 mL each) added every 1.5 hours. Given these findings, the investigation of harsher conditions of organic matter removal was avoided in the present study.

Building on the conditions established by Wohlleben et al. (2023) for organic matrix removal using Fenton reagent, which were designed to ensure compatibility with degradable polymers, this study tested various combinations of H_2O_2 (35%) and $FeSO_4$ (15 mg/mL and 20 mg/mL) ranging from 5x5 mL to 5x25 mL. Most of the experiments were done at room temperature without external heating (see Tab. 1 and SI, Tab. S2). The

objective was to identify the most efficient reactant ratio for compost degradation while avoiding harsh conditions to preserve the integrity of the polymers. Additionally, the approach aimed to optimise the required time to accelerate the overall extraction process.

5.1.1 Mass Loss Analysis

The extraction method of Wohlleben et al., as described in the supplementary information of their study [79], was tested to establish a benchmark for comparison. To ensure consistency and enable direct comparison with other treatments in this study, the same laboratory equipment and chemicals were used. In a separate study, Fenton's reagent was applied with a 1:1 reactant ratio of $FeSO_4$ (20 mg/mL), added initially and H_2O_2 (30%), added continuously. Further additions were made until no further reaction was observed, although the exact amounts used were not specified [21]. This method achieved a mass reduction of 6.81% ± 1.56% for soil samples and 43.8% ± 6.61% for sludge samples.

The optimal Fenton treatment for MP extraction in this study was identified through systematic testing of various procedures and concentrations based on the evaluation of mass and TOC removal (%). To minimise hydrogen peroxide decomposition and limit violent reactions, the Fenton procedure was performed at room temperature, maintaining reaction temperatures ≤ 50 °C. One of the most promising reagent ratios was 10 mL H_2O_2 (35%) and 10 mL $FeSO_4$ solution (0.05 M) added five times at 30-minute intervals under continuous stirring. After 11 replicates, the average mass removal is 36% ± 4%. No other tested combination of H_2O_2 and $FeSO_4$ demonstrated a greater average mass removal than the 10 mL H_2O_2 (35%) and 10 mL $FeSO_4$ (0.05 M) configuration (Fig. 11). The percentage of mass removal served as the primary criterion for selecting samples for subsequent TOC analysis. In the following sections, this reagents combination will be referred to as the optimised Fenton protocol.

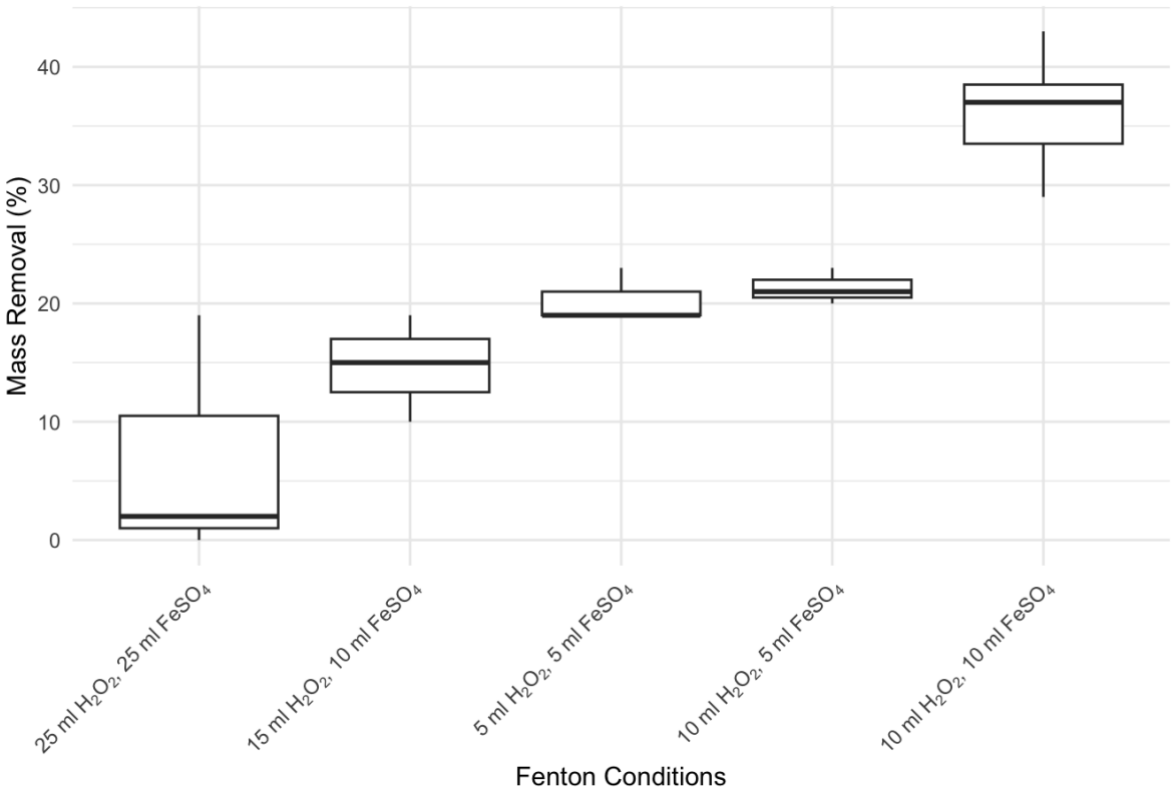

Figure 11: Effect of Fenton reaction conditions on mass removal efficiency. *The plot shows average mass removal from triplicate experiments. H_2O_2 (35%) and $FeSO_4$ (0.05M) were added every 30 minutes (five additions) to 1 g compost in 40 mL Milli-Q water.*

The Wohlleben et al. (2023) method, applied to our compost samples, achieved an average mass reduction of 38% ± 3.5% (Fig. 11). A boxplot is used to visually summarise the distribution, central tendency, and variability of the dataset (Fig. 12). The Wohlleben et al. (2023) method shows a slightly higher mean mass removal percentage (38% ± 3.5%) compared to the optimised Fenton protocol (36% ± 4%). The variability in the results is slightly higher for the optimised Fenton protocol than for the Wohlleben et al. (2023) method. Both methods have outliers. The slight difference in mean mass removal of 2% could be attributed to Fenton's reaction time. According to the MP extraction protocol outlined in Pfohl et al., the Fenton oxidation process took approximately 34 hours in total [78]. In the Wohlleben et al. (2023) method, the reaction time is approximately 25 hours, whereas in the optimised Fenton protocol, it is reduced to 3.5 hours. This indicates that the reaction time was shortened without compromising effectiveness of the Fenton reaction.

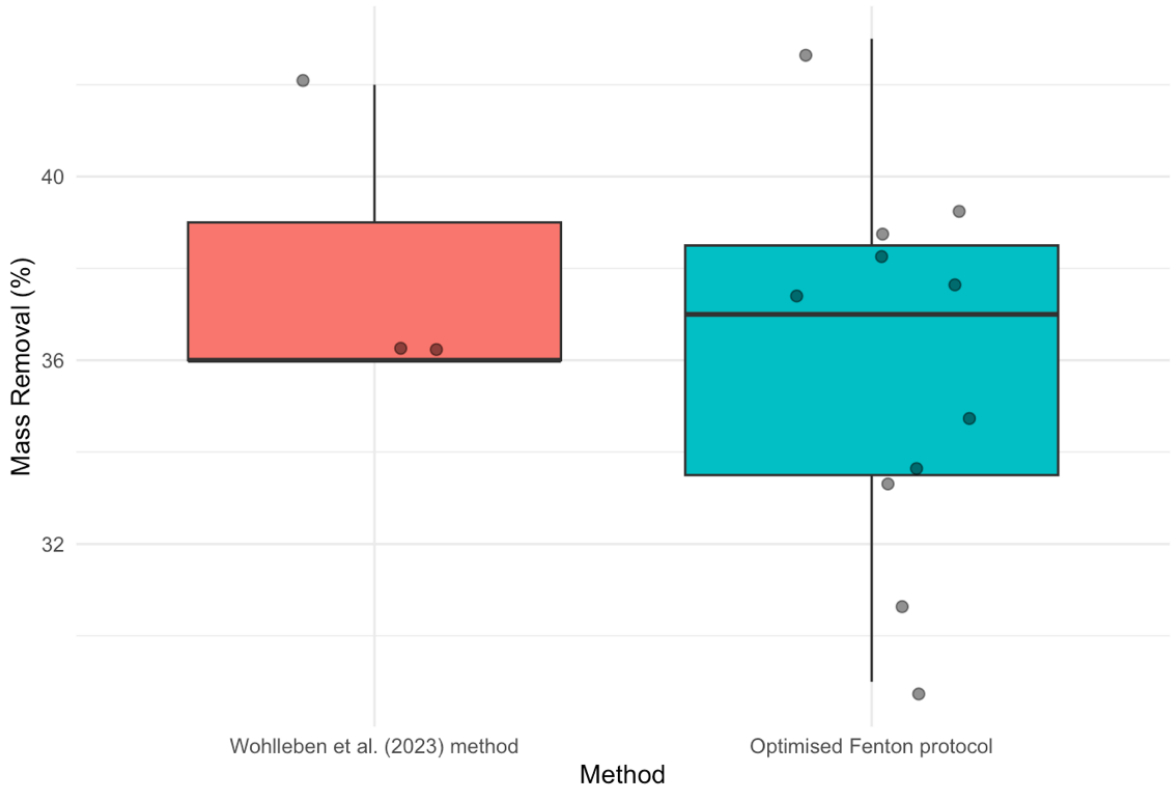

Figure 12: Comparison of the results of mass removal after Fenton treatment between the Wohlleben et al. (2023) method and the optimised Fenton protocol.

In addition, tests were carried out to determine the maximum removal efficiency of organic matter by Fenton without considering its impact on the polymers. This was achieved by employing very high concentrations of H_2O_2 (35%, 5x25 mL) and $FeSO_4$ solution (0.05 M, 5x25 mL), with reaction temperatures reaching 85 °C. The results determined with the weighing method (as described in Chapter 4.1) showed that 6% to 19% of the mass was removed (see SI, Tab. S2). The lower removal efficiencies were observed in samples where no HCl was added after filtration, while the highest efficiencies were found in samples treated with HCl after filtration (cf. Fig. 11). The overall low removal values, especially in comparison to other Fenton reactant proportions, can be attributed to the formation of iron sludge. During the Fenton reaction, ferric hydroxide ($Fe(OH)_3$) forms as a byproduct when Fe^{2+} is oxidised to Fe^{3+}, followed by the hydrolysis of Fe^{3+} [69]. The excessive use of $FeSO_4$ in this experiment led to the generation of a larger quantity of iron sludge, which increased the mass of the material retained on the filter. This outcome highlights a limitation of assessing organic

matrix removal based solely on weight measurements. For this reason, we incorporated TOC analyses for a more precise assessment of the results.

According to Goi & Trapido and Satilmis & Schrader H_2O_2 should be added dropwise to the reaction beaker to assure a constant availability of reactants [85], [86]. A continuous supply of Fe^{2+} ions and H_2O_2 could increase the reaction rate and produce more hydroxyl radicals, thereby enhancing organic matter removal efficiency. For this reason, various test experiments adding H_2O_2 dropwise were performed. The obtained results exhibited variability, making this method difficult to reproduce consistently. Compared to the direct addition method, this approach did not show any significant improvement in organic matter removal and was not further studied. Moreover, the results showed high dispersion and were not consistent between replicates (Fig. 13).

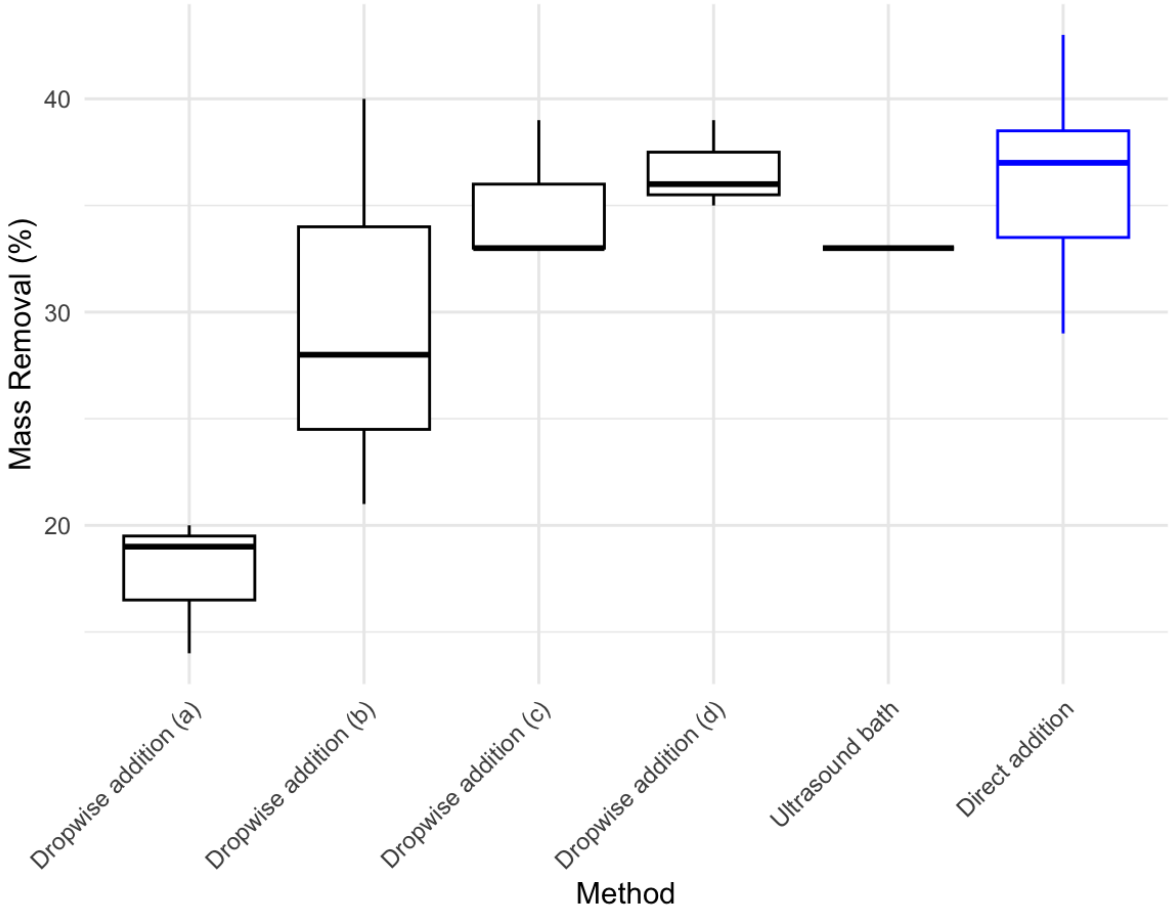

Figure 13: Comparison of mass removal efficiency across different addition methods. Dropwise addition (a): 75 mL H_2O_2 (time independent) and 30 mL $FeSO_4$. Dropwise addition (b): 5x10 mL H_2O_2 and 5x5 mL $FeSO_4$. Direct addition (Optimised Fenton protocol), ultrasound bath, and dropwise addition (c) use 5x10 mL H_2O_2 (35%) and 5x10 mL $FeSO_4$ (0.05M) every 30 minutes. Dropwise addition (d): 5x20 mL H_2O_2 and 5x10 mL $FeSO_4$ every 30 minutes.

Another approach was to place the beaker in an ultrasound bath instead of using magnetic or mechanical stirring. This aimed to enhance reaction kinetics by improving mixing and mass transfer within the solution, potentially increasing the organic matter removal. This method achieved a 33% reduction in mass, determined by the direct weighing method. However, the results were comparable to those obtained with the stirring method, showing no significant advantage over it (Fig. 13).

Alternatively, NaOCl could substitute the Fenton reaction in the organic matter removal. Bottone et al. showed that NaOCl effectively removed soil organic matter without significantly impacting MPs of PP, PLA, LDPE and PET [68]. The surface characterisation of the plastic particles was done with SEM and FTIR. Previous studies have tested the efficacy of 1 M NaOCl with a soil/solution ratio of 1:5 for organic soils in removing organic matter [68], [87]. For this experimental case, we employed the same concentration and ratio, followed by the application of a 2 M NaOCl solution to assess the upper limits of effectiveness. The mass removal determined with the weighing method of the lower concentration was 30%, while that of the higher concentration was 35%. These are lower than those achieved by the Wohlleben et al. (2023) method and the here proposed protocol and, therefore, discarded as an alternative. Additionally, white particles were observed while filtering the NaOCl-compost solution. These particles might be bleached organic material that has not undergone decomposition (Fig. 14). This is particularly evident in the low-concentration sample, which also exhibits a comparably high TOC percentage (see Chapter 5.1.2).

Figure 14: White particles floating on the surface of the residual NaOCl-compost solution during filtration.

5.1.2 Total Organic Carbon Analysis

Given the limitations of the direct weighing/mass loss determination method, namely measurement inaccuracies and external influences on weight fluctuations, such as the amount of $FeSO_4$ solution used in the respective process, this method cannot be considered as sole proof of the degradation of organic matter. Its principal use is to make an initial estimate of effectiveness. This is why an additional carbon analysis has been carried out.

Two distinct organic carbon peaks were observed in the untreated native compost samples: One between 275 °C and 305 °C and another at 500 °C, suggesting the

presence of two types of organic matter with differing thermal stability. The high-intensity secondary peak at 500 °C likely corresponds to refractory organic carbon (Fig. 15).

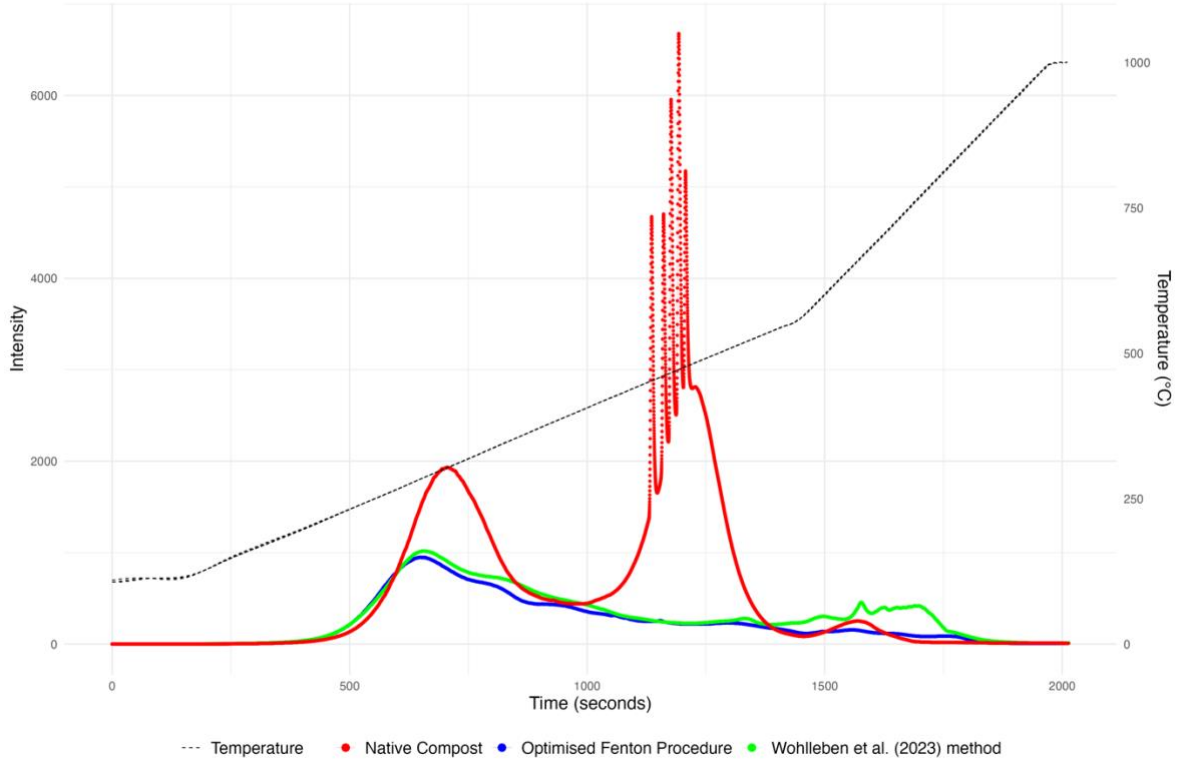

Figure 15: Carbon intensity comparison between a representative sample for Native Compost, the Optimised Fenton Procedure and the Wohlleben et al. (2023) method.

Samples treated with the optimised Fenton protocol or the Wohlleben et al. (2023) method show significantly lower intensities for organic carbon release than untreated compost, indicating effective organic carbon removal. Fenton-treated samples display little to no secondary peaks, suggesting minimal residual carbon content. The smaller peaks observed around 700 °C in both native compost and Fenton-treated samples represent inorganic carbon. It remains to be understood why Fenton treatment removes more refractory organic material while being less effective on thermally labile fractions. One hypothesis is that LECO combustion interacts differently with organic matter than Fenton oxidation. Another possibility is that Fenton oxidation removes the thermally labile fraction while partially degrading the refractory organic carbon. This could cause

a shift in the secondary peaks observed in untreated samples, which consequently disappear in the Fenton-treated samples.

Figure 16 shows the comparison between distributions, central tendencies, and variabilities of TOC percentages across different treatment methods. Native homogenised compost contains an average of 13.88% ± 2.05% TOC. Carbon measurement with LECO confirmed that the main protocols, optimised Fenton protocol and the Wohlleben et al. (2023) method reduce the presence of organic carbon. Samples treated with the Wohlleben et al. (2023) method contain an average of 2.05% ± 0.54% TOC, and the ones treated with the optimised Fenton protocol contain an average of 2.42% ± 0.92% TOC (Fig. 16, see SI for details on individual measurements, Tab. S3). In this context, "optimised" refers to the Fenton protocol's adjusted conditions, which prioritise preserving polymer integrity while achieving effective carbon removal, though with slightly lower efficiency. Two samples from the maximum removal test were analysed for TOC content, resulting in an average of 1.10% ± 0.08% TOC. As anticipated, this value is slightly lower than the average TOC values obtained using the optimised Fenton protocol and the Wohlleben et al. (2023) method. However, isolated samples from the optimised Fenton protocol exhibited even lower TOC values (as low as 0.97%; see SI, Table S3) compared to the minimum TOC value observed in the maximum removal test samples (1.04%). This underscores the effectiveness of the optimised Fenton protocol, as it achieves comparable or superior organic carbon removal while minimising the risk of excessive polymer degradation.

The average TOC removal efficiency is 85.24% ± 3.90% for the Wohlleben et al. (2023) method and 82.53% ± 6.64% for the optimised Fenton protocol. The residual organic carbon may originate from lignin, a key contributor to recalcitrant organic matter in compost [88]. Lignin, a complex component of plant biomass, is derived from sources such as grass, rice straw, tree branches, and pine needles [89], [90]. Due to its chemical structure, which includes aromatic rings, C-O bonds, alkyl groups, hydroxyl groups, and linkages between monomeric units [90], lignin is more resistant to degradation compared to other organic compounds in compost. The remaining material, excluding inorganic carbon, likely consists of non-carbon compounds such as heavy metals,

phosphorus fractions, and nitrogen compounds, which are commonly found in compost [91].

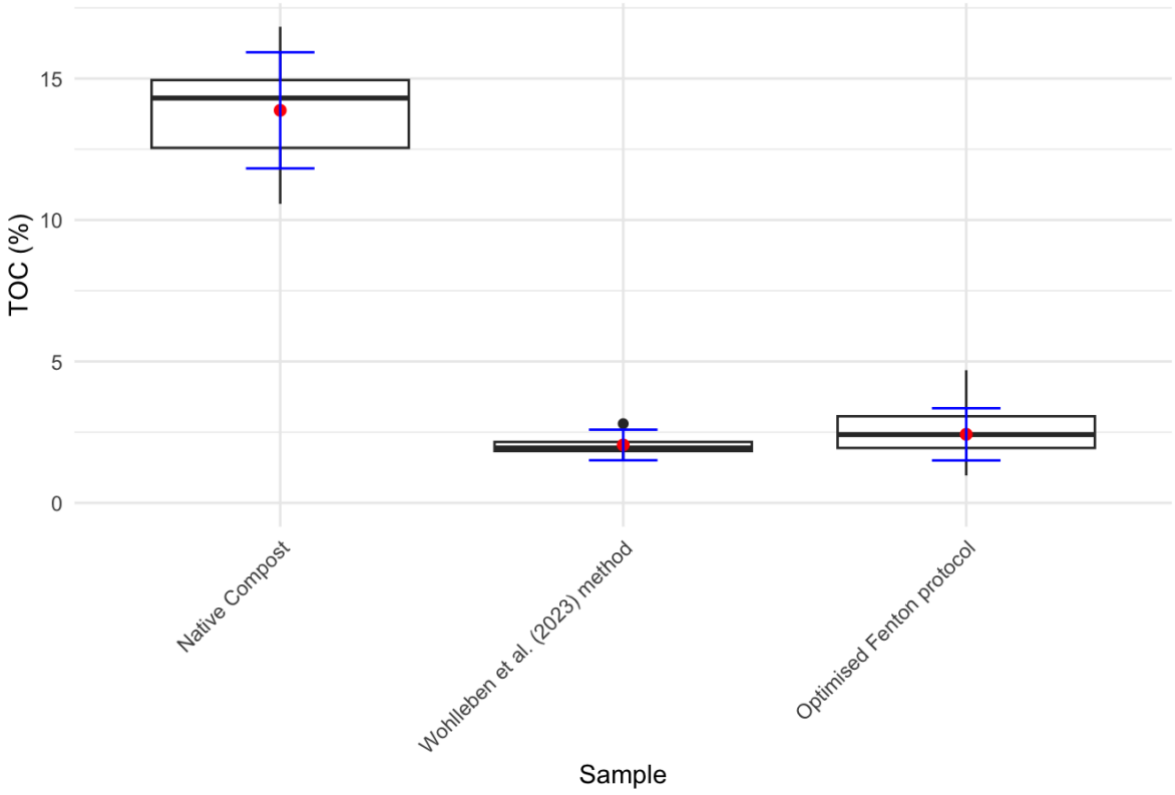

Figure 16: Comparison between the total organic carbon of native compost before and after organic matrix removal methods (Optimised Fenton protocol and Wohlleben et al. (2023) method).

In addition to the TOC analyses of the Fenton protocols, the samples treated with NaOCl were also analysed for TOC. The TOC of the low-concentration (1 M) NaOCl protocol averaged 5.34% ± 0.83%, while that of the high-concentration (2 M) NaOCl protocol averaged 2.58% ± 0.25% (see SI, Fig. S1). These results show that only the NaOCl protocol with the higher concentration is comparable to the Fenton procedures. The increased concentration and harsher conditions pose a risk of attacking the degradable polymers. Therefore, the use of NaOCl was considered a less suitable method for the removal of organic matter.

5.2 Combustible Fraction of Native Compost

The average weight loss/mass removal of the untreated compost is 35.80% ± 4.82% using the high-temperature oven (550 °C, 4 hours) and 34.08% ± 3.53% when using the LECO furnace (ramped from 100 °C to 1000 °C in 32 minutes) (Tab. 2, weights used for the calculation are provided in the SI, Tab. S4). This suggests that the non-combustible matter averages between 64% for the loss-on-ignition (LOI) test and 66% for the non-combustible matter test. Both the optimised Fenton protocol and the Wohlleben et al. (2023) method achieved comparable mass removal efficiencies, with 38% ± 3.5% for the Wohlleben et al. (2023) method and 36% ± 4% for the optimised Fenton protocol (Fig. 11). The comparison between the results for the combustible fraction and the Fenton treatments highlights that the latter decomposes organic material with high efficiency. If the percentage of the non-combustible matter from the LOI test is used as a baseline for potential degradation rates, the optimised Fenton protocol proves to be well-suited. It demonstrates a strong capacity for organic matrix removal.

Table 2: Results of the combustible fraction of native compost. Mass removal was calculated based on the difference in mass before and after combustion.

Combustible matter (%) LOI test	Combustible matter (%) LECO
30.00	30.38
40.00	37.42
32.00	34.43
41.00	-
36.00	-
Avg. **35.80 ± 4.82**	*Avg.* **34.08 ± 3.53**

5.3 Impact of the Optimised Fenton Protocol on the Integrity of Biodegradable Polymers

The following statements and statistics are based on digital optical microscope images analysed using Fiji [80], followed by statistical analysis with RStudio [81].

The median (D50), D10, and D90 are used in this study to analyse differences in particle size (Tab. 3). Due to high variability in the particle size distribution of the initial sample, the mean and standard deviation are unreliable for tracking changes in particle size. These metrics (D10, D50, D90) provide a clearer understanding and help identify selective changes in specific size fractions of the MPs used. Additionally, histograms are used to describe the shape of the size distribution (Fig. 17).

The area of individual particles was determined using an automated add-on of Fiji [80]. Later, the area was converted to an equivalent diameter (assuming circular particles) to ease the understanding and relate to the particle fraction that was used in the experiment. Although this method introduces a degree of imprecision due to the assumption of circular particles, it was considered an acceptable approximation for this analysis. Generally, the standard deviation measures the spread around a mean value, but percentiles like D10, D50, and D90 represent specific points in a distribution, not averages. While these percentiles indicate data spread, it is not possible to directly calculate a standard deviation for them. To estimate variability around D10, D50, and D90, bootstrapping can be employed, particularly when the data deviate from a normal distribution, as is the case here. Bootstrapping repeatedly samples the original data with replacement, calculating D10, D50, and D90 for each resample. After multiple iterations, the variability in these values provides an estimate of the standard deviation for each percentile. The complete R-scripts, including the bootstrapping, can be found in the appendix.

Previous studies have found that ultrasonication applied to soils does not affect MP size distribution, including PBAT [92]. These findings could be applied to compost, making it

a suitable method to disperse MPs in water, break up agglomerates of compost and MPs and therefore allow a more effective Fenton treatment as well as density separation.

Table 3: Percentiles (D10, median D50, D90 with Area converted to diameter) describing the size distribution of the PLA and PBAT particles in pristine status, after sonication only, after Optimised Fenton treatment only and after the complete procedure (sonication and Fenton). Results are presented as percentiles (D10, D50 and D90) ± bootstrapped SD.

Material	Conditions	D10 [µm]	D50 [µm]	D90 [µm]
PLA	Pristine	64.85 ± 2.60	140.54 ± 11.05	252.21 ± 10.54
	Sonication	65.22 ± 3.66	128.91 ± 8.81	296.05 ± 21.80
	Fenton	61.74 ± 1.11	115.24 ± 16.09	263.57 ± 12.45
	Complete	59.63 ± 1.67	98.02 ± 10.46	253.24 ± 12.75
PBAT	Pristine	61.46 ± 1.42	108.11 ± 6.46	221.15 ± 12.57
	Sonication	62.63 ± 2.93	123.84 ± 8.53	236.76 ± 18.81
	Fenton	60.09 ± 1.29	101.09 ± 7.43	213.29 ± 12.16
	Complete	58.26 ± 1.14	80.70 ± 5.31	184.59 ± 36.29

For PLA, sonication alone slightly reduces the median particle size (D50) but increases the size of the largest particles (D90) (Tab. 3), which we believe could be due to the variability of the initial sample. Fenton treatment alone reduces median size more than sonication alone but also increases the size of some larger particles. Complete treatment reduces the median size and maintains the D10 and D90 close to the pristine state, with only minor changes considering the bootstrapped SD. This indicates that although the central tendency of particle size shifts, the overall size distribution remains stable.

In the case of PBAT, sonication leads to an increase in both the median and D90, likely due to the initial sample's variability. The size changes observed here are consistent with the findings of Büks et al. [92] and likely arise from natural variability in particle sizes. Fenton treatment results in a slight reduction in particle sizes, which is closer to the pristine state compared to sonication alone. Complete treatment reduces the size of particles in all the analysed percentiles.

The size reduction of PLA from pristine state to complete treatment is 8.05% for D10, 30.28% for D50, and -0.41% (slight increase) for D90. For PBAT, the size reduction from pristine state to complete treatment is 5.21% for D10, 25.37% for D50, and 16.54% for D90. For both PLA and PBAT, medium particles (D50) are affected the most, showing the largest percentage reductions in size. The small particle fraction (D10) experiences the least reduction, and large particles (D90) show varying degrees of reduction or even a slight increase. If the treatment damages the particles, we anticipate that smaller particles will be more affected than larger ones. This is because smaller particles have a larger surface area relative to their volume, providing more surface for reactive oxygen species to attack. We do not observe such a behaviour, suggesting a stability of the particles when they are treated with Fenton in the proposed proportions in this work.

PLA experiences a more substantial reduction in the median particle size (D50). This could imply that the degradation process is more selective, potentially breaking down larger particles more effectively. PBAT appears to follow a different degradation pathway as it is more uniformly affected across the entire particle size distribution by the complete treatment, making it the polymer more affected overall by this treatment. This could also suggest a potentially more consistent and predictable environmental behaviour of PBAT. Both polymers show relative stability across the D10 and D90 percentiles without a significant reduction in size for the treatment that is applied in this work.

A previous study by Pfohl et al. reported that the Fenton protocol led to a reduction in D50 size of 6.2% ± 1.7% for PLA particles and 6.9% ± 2.7% for PBAT particles [78]. In comparison, our study observed a more significant reduction in D50 size, ranging from about 25% to 30%. One potential reason for this discrepancy could be the difference in analytical methods. Pfohl et al. used Fraunhofer light scattering, whereas our study employed digital optical microscopy and indirect processing software. Although our method may be less precise in terms of measurement resolution, laser diffraction techniques are heavily weighted towards larger particles due to the scattering intensity scaling with particle size. This could potentially lead to an underestimation of the reduction in particle size if smaller fragments dominate the changes. In contrast, digital optical microscopy and the analysis with Fiji may be more sensitive to smaller

fragments, leading to a larger observed reduction in D50 size. Another origin of the observed difference could be the reagent concentration employed in the studies. Pfohl et al. used a lower concentration of iron sulphate (2.5 g/L) than the 15 g/L used here but a higher H_2O_2 concentration (250 g/L compared to 195 g/L in this study).

The results of the D10, D50, and D90 analysis combined with a statistical test can provide complementary insights into particle size distributions. The original data set does not follow a normal distribution (Fig. 15), necessitating the use of a non-parametric test, specifically the Mann-Whitney U test, to assess the statistical significance of the observed differences in particle size distributions between samples. It evaluates overall differences between distributions, offering a broad comparison of their shapes. Unlike parametric tests, the Mann-Whitney U test compares medians rather than means and is less affected by outliers. This makes it suitable for the high variability observed in particle size distributions.

The p-values calculated at a significance level of 95% suggest that there is no significant difference between the particle size distributions of the samples. This indicates that after a complete treatment of sonication followed by Fenton oxidation, the integrity of the polymers is maintained. The only comparison showing a significant difference ($p = 0.0041$) was observed between pristine PBAT and PBAT after complete treatment, as the p-value was below 0.05. However, this difference may be due to sample-specific variations, as no significant differences were observed between pristine PBAT and PBAT after sonication ($p = 0.2102$) or the Fenton reaction ($p = 0.5652$) (see SI, Tab. S1 for details). This may indicate that the observed difference is linked to natural variability in particle size distributions, rather than extensive degradation caused by the complete treatment process. These findings support the conclusion that polymer integrity is preserved after the complete treatment regimen.

It is important to notice that the experiments presented here are a worst-case scenario for polymers. Hydroxyl radicals generated by the Fenton reagent react with the most accessible and reactive sites. The organic matter in the compost samples typically has a large surface area and contains various functional groups that are highly reactive to hydroxyl radicals [93]. It is, therefore, likely that the organic matter of the compost will be oxidised more rapidly and extensively. This also means that there is less time and

less amount of reactive oxygen species that can affect the polymers if an environmental matrix (compost) is included rather than just allowing the Fenton reagent to react with the polymers. Therefore, there is a possibility that the effect we observed on the polymers in this study could be reduced if the optimised Fenton treatment for the extraction of microplastics from compost is used in further research.

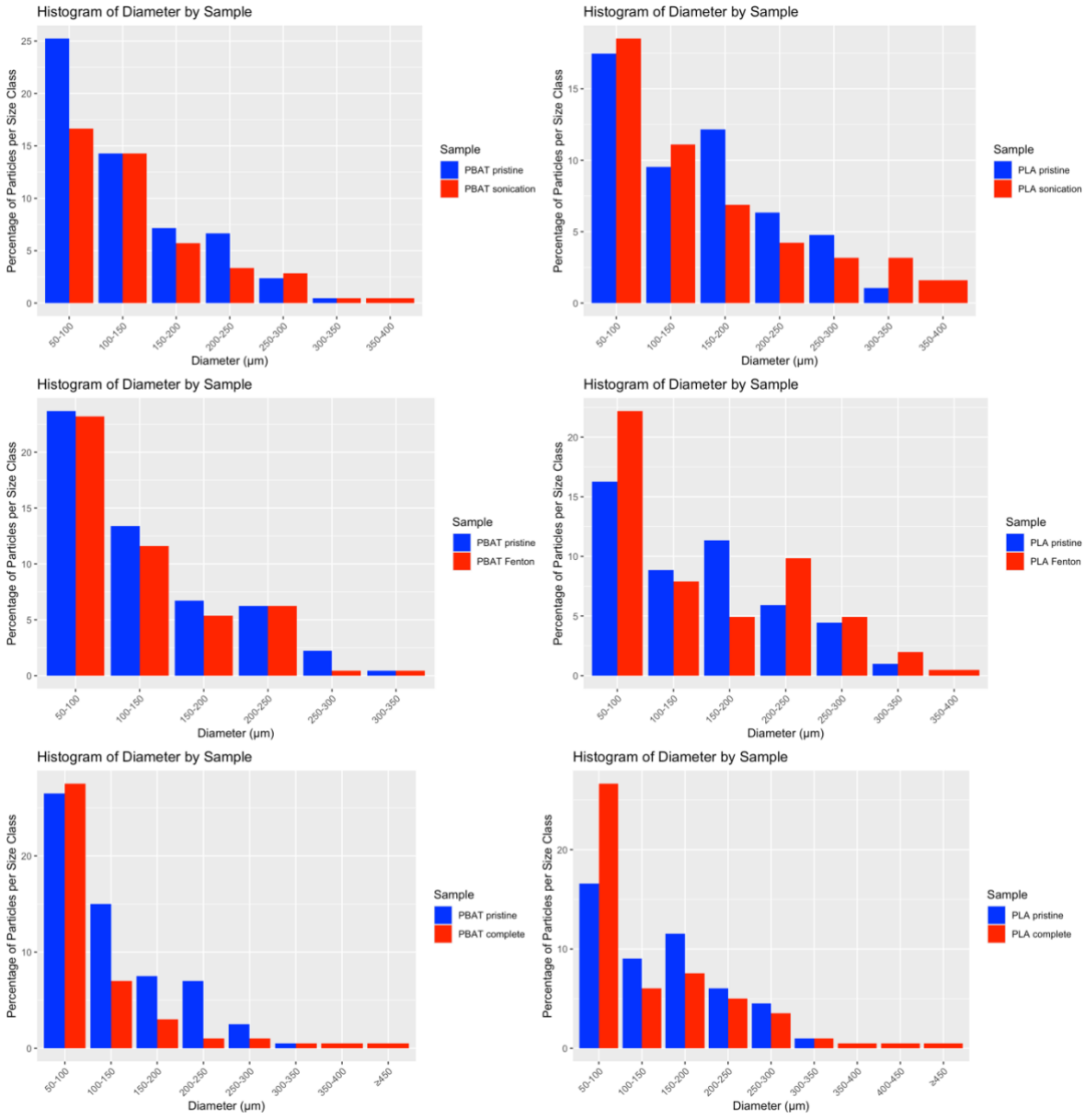

Figure 17: Histograms of the size distribution of the polymer particles. Comparison between pristine condition and after either sonication only, Fenton only or complete treatment (Fenton and sonication).

6 Conclusions and Environmental Implications

In this study, we developed and evaluated a protocol to remove organic matter as part of an extraction method for microplastics from complex compost matrices, with a focus on biodegradable plastics like PLA and PBAT. The aim was to maximise organic matter removal while preserving polymer integrity for subsequent analysis. Building on prior research, particularly the method introduced by Wohlleben et al. [79], the presented protocol employs Fenton oxidation as the primary mechanism. The efficiency of the protocol was assessed through a series of experiments, including mass loss determination, TOC measurements before and after treatment, and analysis of the combustible fraction of the compost. Results were compared to the Wohlleben et al. (2023) method and an alternative approach using NaOCl oxidation, as proposed by Bottone et al. [68].

The presented protocol uses a 1:1 reagent ratio, with 10 mL H_2O_2 (35%) and 10 mL $FeSO_4$ (0.05 M) per dose. A total of 5 doses are administered, with each dose added every 30 minutes to a compost-MilliQ solution at a pH of approximately 3. The method demonstrates high effectiveness in removing organic matter from environmental samples that could contain MPs. The presented protocol achieves an average mass removal of 36% ± 4%, which is close to the 36% ± 5% achieved by the combustion of the sample. Further mass removal may not be feasible, as LOI and LECO carbon analyser measurements show that the non-combustible matter in compost, which persists even at temperatures up to 1000 °C in LECO analysis, ranged between 64% and 66%. This method facilitates the extraction of MPs from complex organic matrices for further analysis.

The measurement of TOC shows that an average of 82.53% ± 6.64% of the organic carbon is removed by the presented method. Even under increased reagent concentration and external heating, a complete removal of organic matter is not achieved. A comparable organic matrix removal protocol for MP analysis, introduced by Wohlleben et al. [79], shows similar results, with less than a 1% difference in remaining TOC after treatment. While the Wohlleben et al. (2023) method requires approximately

25-26 hours, the here-introduced protocol completes the process in under 4 hours. Shorter processing times reduce labour costs and enable higher throughput, making the method suitable for industrial-scale applications.

In comparison, NaOCl is less effective than Fenton oxidation for organic matter removal from compost samples. Although high concentrations of NaOCl produce comparable results, these concentrations pose a risk of damaging MPs, making NaOCl less suitable for MP extraction. The presented protocol causes a slight reduction in the size of PLA and PBAT particles. However, statistical analysis reveals no significant difference in particle size distribution before and after treatment. This finding aligns with previous studies [78], [79], which also reported minor reductions in particle size following treatment. This indicates that the presented method could effectively extract degradable plastics without significantly altering their size.

The presented method holds significant advantage for biodegradable plastic manufacturers and research institutions. By preserving the integrity of degradable plastics during extraction, it enables a more accurate assessment of their degradation kinetics in compost environments. This is particularly important since compost is often applied as fertiliser on agricultural fields. Additionally, the presented protocol provides a reliable, less destructive extraction method for monitoring microplastic in compost. This supports the development of industrial fully biodegradable plastics production and facilitates the establishment of improved standards for their use and disposal.

In conclusion, the method introduced in this study offers broad industrial and environmental applications. It provides a cost-effective, time-efficient, and scalable solution for the analysis and development of degradable plastics, which is fundamental in the transition toward a greener, more sustainable future.

7 References

[1] M. MacLeod, H. P. H. Arp, M. B. Tekman, and A. Jahnke, “The global threat from plastic pollution,” *Science*, vol. 373, no. 6550, pp. 61–65, Jul. 2021, doi: 10.1126/science.abg5433.

[2] Statista Research Department, “Global plastic production,” Statista. Accessed: Sep. 15, 2024. [Online]. Available: https://www.statista.com/statistics/282732/global-production-of-plastics-since-1950/

[3] S. Allen *et al.*, “Atmospheric transport and deposition of microplastics in a remote mountain catchment,” *Nat. Geosci.*, vol. 12, no. 5, pp. 339–344, May 2019, doi: 10.1038/s41561-019-0335-5.

[4] S. B. Borrelle *et al.*, “Predicted growth in plastic waste exceeds efforts to mitigate plastic pollution,” *Science*, vol. 369, no. 6510, pp. 1515–1518, Sep. 2020, doi: 10.1126/science.aba3656.

[5] R. Geyer, J. R. Jambeck, and K. L. Law, “Production, use, and fate of all plastics ever made,” *Sci. Adv.*, vol. 3, no. 7, p. e1700782, Jul. 2017, doi: 10.1126/sciadv.1700782.

[6] T. Hofmann *et al.*, “Plastics can be used more sustainably in agriculture,” *Commun. Earth Environ.*, vol. 4, no. 1, p. 332, Sep. 2023, doi: 10.1038/s43247-023-00982-4.

[7] A. Chamas *et al.*, “Degradation Rates of Plastics in the Environment,” *ACS Sustain. Chem. Eng.*, vol. 8, no. 9, pp. 3494–3511, Mar. 2020, doi: 10.1021/acssuschemeng.9b06635.

[8] S. Zeytin *et al.*, “Quantifying microplastic translocation from feed to the fillet in European sea bass Dicentrarchus labrax,” *Mar. Pollut. Bull.*, vol. 156, p. 111210, Jul. 2020, doi: 10.1016/j.marpolbul.2020.111210.

[9] A. Ragusa *et al.*, “Plasticenta: First evidence of microplastics in human placenta,” *Environ. Int.*, vol. 146, p. 106274, Jan. 2021, doi: 10.1016/j.envint.2020.106274.

[10] C. Chen *et al.*, “Microplastics in the Bronchoalveolar Lavage Fluid of Chinese Children: Associations with Age, City Development, and Disease Features,” *Environ. Sci. Technol.*, vol. 57, no. 34, pp. 12594–12601, Aug. 2023, doi: 10.1021/acs.est.3c01771.

[11] N. S. Roslan *et al.*, “Detection of microplastics in human tissues and organs: A scoping review,” *J. Glob. Health*, vol. 14, p. 04179, Aug. 2024, doi: 10.7189/jogh.14.04179.

[12] *Dietary and Inhalation Exposure to Nano- and Microplastic Particles and Potential Implications for Human Health*, 1st ed. Geneva: World Health Organization, 2022.

[13] S. Castan, C. Henkel, T. Hüffer, and T. Hofmann, “Microplastics and nanoplastics barely enhance contaminant mobility in agricultural soils,” *Commun. Earth Environ.*, vol. 2, no. 1, p. 193, Sep. 2021, doi: 10.1038/s43247-021-00267-8.

[14] A. Rudin and P. Choi, *The elements of polymer science and engineering*. Academic press, 2012.

[15] S. Thakur, J. Chaudhary, B. Sharma, A. Verma, S. Tamulevicius, and V. K. Thakur, “Sustainability of bioplastics: Opportunities and challenges,” *Curr. Opin. Green Sustain. Chem.*, vol. 13, pp. 68–75, Oct. 2018, doi: 10.1016/j.cogsc.2018.04.013.

[16] J. Martínez-Blanco *et al.*, “Compost benefits for agriculture evaluated by life cycle assessment. A review,” *Agron. Sustain. Dev.*, vol. 33, no. 4, pp. 721–732, Oct. 2013, doi: 10.1007/s13593-013-0148-7.

[17] M. Diacono and F. Montemurro, “Long-term effects of organic amendments on soil fertility. A review,” *Agron. Sustain. Dev.*, vol. 30, no. 2, pp. 401–422, Apr. 2010, doi: 10.1051/agro/2009040.

[18] Recycled Organics Unit, The University of New South Wales, “Life Cycle Inventory and Life Cycle Assessment for Windrow Composting Systems,” 2006. Accessed: Jan. 03, 2025. [Online]. Available: https://www.epa.nsw.gov.au/-/media/epa/corporate-site/resources/warrlocal/060400-windrow-assess.pdf

[19] A. Boldrin, J. K. Andersen, J. Møller, T. H. Christensen, and E. Favoino, “Composting and compost utilization: accounting of greenhouse gases and global warming contributions,” *Waste Manag. Res.*, vol. 27, no. 8, pp. 800–812, Nov. 2009, doi: 10.1177/0734242X09345275.

[20] G. Bonanomi, V. Antignani, C. Pane, and F. Scala, “Suppression of Soilborne Fungal Diseases with Organic Amendments,” *J. Plant Pathol.*, vol. 89, no. 3, pp. 311–324, 2007.

[21] R. R. Hurley, A. L. Lusher, M. Olsen, and L. Nizzetto, “Validation of a Method for Extracting Microplastics from Complex, Organic-Rich, Environmental Matrices,”

Environ. Sci. Technol., vol. 52, no. 13, pp. 7409–7417, Jul. 2018, doi: 10.1021/acs.est.8b01517.

[22] D. Ortiz, M. Munoz, J. Nieto-Sandoval, C. Romera-Castillo, Z. M. De Pedro, and J. A. Casas, "Insights into the degradation of microplastics by Fenton oxidation: From surface modification to mineralization," *Chemosphere*, vol. 309, p. 136809, Dec. 2022, doi: 10.1016/j.chemosphere.2022.136809.

[23] United Nations, "Transforming our world: the 2030 Agenda for Sustainable Development | Department of Economic and Social Affairs." Accessed: Sep. 15, 2024. [Online]. Available: https://sdgs.un.org/2030agenda

[24] A. Stubbins, K. L. Law, S. E. Muñoz, T. S. Bianchi, and L. Zhu, "Plastics in the Earth system," *Science*, vol. 373, no. 6550, pp. 51–55, Jul. 2021, doi: 10.1126/science.abb0354.

[25] M. Cole, P. Lindeque, C. Halsband, and T. S. Galloway, "Microplastics as contaminants in the marine environment: A review," *Mar. Pollut. Bull.*, vol. 62, no. 12, pp. 2588–2597, Dec. 2011, doi: 10.1016/j.marpolbul.2011.09.025.

[26] A. G. Anderson, J. Grose, S. Pahl, R. C. Thompson, and K. J. Wyles, "Microplastics in personal care products: Exploring perceptions of environmentalists, beauticians and students," *Mar. Pollut. Bull.*, vol. 113, no. 1–2, pp. 454–460, Dec. 2016, doi: 10.1016/j.marpolbul.2016.10.048.

[27] L. M. Hernandez, N. Yousefi, and N. Tufenkji, "Are There Nanoplastics in Your Personal Care Products?," *Environ. Sci. Technol. Lett.*, vol. 4, no. 7, pp. 280–285, Jul. 2017, doi: 10.1021/acs.estlett.7b00187.

[28] K. Waldschläger, S. Lechthaler, G. Stauch, and H. Schüttrumpf, "The way of microplastic through the environment – Application of the source-pathway-receptor model (review)," *Sci. Total Environ.*, vol. 713, p. 136584, Apr. 2020, doi: 10.1016/j.scitotenv.2020.136584.

[29] A. van Wezel, I. Caris, and S. A. E. Kools, "Release of primary microplastics from consumer products to wastewater in the Netherlands," *Environ. Toxicol. Chem.*, vol. 35, no. 7, pp. 1627–1631, 2016, doi: 10.1002/etc.3316.

[30] G. Rajeshkumar *et al.*, "Environment friendly, renewable and sustainable poly lactic acid (PLA) based natural fiber reinforced composites – A comprehensive

review," *J. Clean. Prod.*, vol. 310, p. 127483, Aug. 2021, doi: 10.1016/j.jclepro.2021.127483.

[31] M. S. Singhvi, S. S. Zinjarde, and D. V. Gokhale, "Polylactic acid: synthesis and biomedical applications," *J. Appl. Microbiol.*, vol. 127, no. 6, pp. 1612–1626, Dec. 2019, doi: 10.1111/jam.14290.

[32] T. A. Swetha *et al.*, "A review on biodegradable polylactic acid (PLA) production from fermentative food waste - Its applications and degradation," *Int. J. Biol. Macromol.*, vol. 234, p. 123703, Apr. 2023, doi: 10.1016/j.ijbiomac.2023.123703.

[33] L. McKeen, "12 - Renewable Resource and Biodegradable Polymers," in *The Effect of Sterilization on Plastics and Elastomers (Third Edition)*, L. McKeen, Ed., Boston: William Andrew Publishing, 2012, pp. 305–317. doi: 10.1016/B978-1-4557-2598-4.00012-5.

[34] X. Pang, X. Zhuang, Z. Tang, and X. Chen, "Polylactic acid (PLA): Research, development and industrialization," *Biotechnol. J.*, vol. 5, no. 11, pp. 1125–1136, Nov. 2010, doi: 10.1002/biot.201000135.

[35] A. Södergård and M. Stolt, "Properties of lactic acid based polymers and their correlation with composition," *Prog. Polym. Sci.*, vol. 27, no. 6, pp. 1123–1163, Jul. 2002, doi: 10.1016/S0079-6700(02)00012-6.

[36] A. Bhatia, "Compatibility of biodegradable poly (lactic acid) (PLA) and poly (butylene succinate) (PBS) blends for packaging application," 2007.

[37] C. Luo *et al.*, "Comparative life cycle assessment of PBAT from fossil-based and second-generation generation bio-based feedstocks," *Sci. Total Environ.*, vol. 954, p. 176421, Dec. 2024, doi: 10.1016/j.scitotenv.2024.176421.

[38] B. K. Ratshoshi, S. Farzad, and J. F. Görgens, "A techno-economic study of Polybutylene adipate terephthalate (PBAT) production from molasses in an integrated sugarcane biorefinery," *Food Bioprod. Process.*, vol. 145, pp. 11–20, May 2024, doi: 10.1016/j.fbp.2024.01.011.

[39] Y. Yang *et al.*, "Complete bio-degradation of poly(butylene adipate-co-terephthalate) via engineered cutinases," *Nat. Commun.*, vol. 14, no. 1, p. 1645, Mar. 2023, doi: 10.1038/s41467-023-37374-3.

[40] Chemanalyst, “Global PBAT production,” Chemanalyst. Accessed: Nov. 14, 2024. [Online]. Available: https://www.chemanalyst.com/industry-report/polybutylene-adipate-terephthalate-market-655

[41] Y. Cai, J. Lv, and J. Feng, “Spectral Characterization of Four Kinds of Biodegradable Plastics: Poly (Lactic Acid), Poly (Butylenes Adipate-Co-Terephthalate), Poly (Hydroxybutyrate-Co-Hydroxyvalerate) and Poly (Butylenes Succinate) with FTIR and Raman Spectroscopy,” *J. Polym. Environ.*, vol. 21, no. 1, pp. 108–114, Mar. 2013, doi: 10.1007/s10924-012-0534-2.

[42] J. Jian, Z. Xiangbin, and H. Xianbo, “An overview on synthesis, properties and applications of poly(butylene-adipate-*co*-terephthalate)–PBAT,” *Adv. Ind. Eng. Polym. Res.*, vol. 3, no. 1, pp. 19–26, Jan. 2020, doi: 10.1016/j.aiepr.2020.01.001.

[43] H. Ye, Q. Li, J. Li, D. Li, and Z. Ao, “Review on the abiotic degradation of biodegradable plastic poly(butylene adipate-terephthalate): Mechanisms and main factors of the degradation,” *Chin. Chem. Lett.*, p. 109861, Apr. 2024, doi: 10.1016/j.cclet.2024.109861.

[44] M. Agarwal, K. W. Koelling, and J. J. Chalmers, “Characterization of the Degradation of Polylactic Acid Polymer in a Solid Substrate Environment,” *Biotechnol. Prog.*, vol. 14, no. 3, pp. 517–526, Jun. 1998, doi: 10.1021/bp980015p.

[45] R. G. Sinclair, “The Case for Polylactic Acid as a Commodity Packaging Plastic,” *J. Macromol. Sci. Part A*, vol. 33, no. 5, pp. 585–597, May 1996, doi: 10.1080/10601329608010880.

[46] A. N. Mistry *et al.*, “Bioaugmentation with a defined bacterial consortium: A key to degrade high molecular weight polylactic acid during traditional composting,” *Bioresour. Technol.*, vol. 367, p. 128237, Jan. 2023, doi: 10.1016/j.biortech.2022.128237.

[47] P. D. Dissanayake *et al.*, “Effects of biodegradable poly(butylene adipate-co-terephthalate) and poly(lactic acid) plastic degradation on soil ecosystems,” *Soil Use Manag.*, vol. 40, no. 2, p. e13055, Apr. 2024, doi: 10.1111/sum.13055.

[48] N. Nomadolo, O. E. Dada, A. Swanepoel, T. Mokhena, and S. Muniyasamy, “A Comparative Study on the Aerobic Biodegradation of the Biopolymer Blends of Poly(butylene succinate), Poly(butylene adipate terephthalate) and Poly(lactic acid),” *Polymers*, vol. 14, no. 9, p. 1894, May 2022, doi: 10.3390/polym14091894.

[49] M. Raviv *et al.*, “High-nitrogen compost as a medium for organic container-grown crops,” *Bioresour. Technol.*, vol. 96, no. 4, pp. 419–427, Mar. 2005, doi: 10.1016/j.biortech.2004.06.001.

[50] Roman, Martinez, MM, and Pantoja, A, *Farmer’s Compost Handbook: Experiences in Latin America*. 2015.

[51] A. Hassen, K. Belguith, N. Jedidi, A. Cherif, M. Cherif, and A. Boudabous, “Microbial characterization during composting of municipal solid waste,” *Bioresour. Technol.*, vol. 80, no. 3, pp. 217–225, Dec. 2001, doi: 10.1016/S0960-8524(01)00065-7.

[52] F. Adani, P. L. Genevini, F. Gasperi, and F. Tambone, “Composting And Humification,” *Compost Sci. Util.*, vol. 7, no. 1, pp. 24–33, Jan. 1999, doi: 10.1080/1065657X.1999.10701949.

[53] K. Azim, B. Soudi, S. Boukhari, C. Perissol, S. Roussos, and I. Thami Alami, “Composting parameters and compost quality: a literature review,” *Org. Agric.*, vol. 8, no. 2, pp. 141–158, Jun. 2018, doi: 10.1007/s13165-017-0180-z.

[54] J. L. Smith and H. P. Collins, “17 - MANAGEMENT OF ORGANISMS AND THEIR PROCESSES IN SOILS,” in *Soil Microbiology, Ecology and Biochemistry (Third Edition)*, E. A. PAUL, Ed., San Diego: Academic Press, 2007, pp. 471–502. doi: 10.1016/B978-0-08-047514-1.50021-4.

[55] R. Rynk *et al.*, “On-farm composting handbook (NRAES 54),” 1992.

[56] J. B. Gurtler, M. P. Doyle, M. C. Erickson, X. Jiang, P. Millner, and M. Sharma, “Composting To Inactivate Foodborne Pathogens for Crop Soil Application: A Review,” *J. Food Prot.*, vol. 81, no. 11, pp. 1821–1837, Nov. 2018, doi: 10.4315/0362-028X.JFP-18-217.

[57] Statistisches Bundesamt, “Water management: Disposal of sewage sludge from biological waste water treatment, 2021,” Federal Statistical Office. Accessed: Nov. 15, 2024. [Online]. Available: https://www.destatis.de/EN/Themes/Society-Environment/Environment/Water-Management/Tables/ks-16a-public-waste-water-disposal-sewage-sludge-biological-waste-water-treatment-2021.html

[58] European Commission, “Proposal for a DIRECTIVE OF THE EUROPEAN PARLIAMENT AND OF THE COUNCIL concerning urban wastewater treatment (recast).” Accessed: Nov. 11, 2024. [Online]. Available: https://eur-lex.europa.eu/legal-content/EN/TXT/?uri=CELEX:52022PC0541

[59] H. Brťková *et al.*, “Plastic particles in urban compost and their grain size distribution,” *Environ. Pollut.*, vol. 351, p. 124025, Jun. 2024, doi: 10.1016/j.envpol.2024.124025.

[60] M. Braun, M. Mail, R. Heyse, and W. Amelung, “Plastic in compost: Prevalence and potential input into agricultural and horticultural soils,” *Sci. Total Environ.*, vol. 760, p. 143335, Mar. 2021, doi: 10.1016/j.scitotenv.2020.143335.

[61] C. Edo, F. Fernández-Piñas, and R. Rosal, “Microplastics identification and quantification in the composted Organic Fraction of Municipal Solid Waste,” *Sci. Total Environ.*, vol. 813, p. 151902, Mar. 2022, doi: 10.1016/j.scitotenv.2021.151902.

[62] C. Scopetani, D. Chelazzi, A. Cincinelli, T. Martellini, V. Leiniö, and J. Pellinen, “Hazardous contaminants in plastics contained in compost and agricultural soil,” *Chemosphere*, vol. 293, p. 133645, Apr. 2022, doi: 10.1016/j.chemosphere.2022.133645.

[63] V. Hidalgo-Ruz, L. Gutow, R. C. Thompson, and M. Thiel, “Microplastics in the Marine Environment: A Review of the Methods Used for Identification and Quantification,” *Environ. Sci. Technol.*, vol. 46, no. 6, pp. 3060–3075, Mar. 2012, doi: 10.1021/es2031505.

[64] M. Bläsing and W. Amelung, “Plastics in soil: Analytical methods and possible sources,” *Sci. Total Environ.*, vol. 612, pp. 422–435, Jan. 2018, doi: 10.1016/j.scitotenv.2017.08.086.

[65] M. M. Maw, N. Boontanon, S. Fujii, and S. K. Boontanon, “Rapid and efficient removal of organic matter from sewage sludge for extraction of microplastics,” *Sci. Total Environ.*, vol. 853, p. 158642, Dec. 2022, doi: 10.1016/j.scitotenv.2022.158642.

[66] S. S. Monteiro *et al.*, “A straightforward method for microplastic extraction from organic-rich freshwater samples,” *Sci. Total Environ.*, vol. 815, p. 152941, Apr. 2022, doi: 10.1016/j.scitotenv.2022.152941.

[67] F. Radford, L. M. Zapata-Restrepo, A. A. Horton, M. D. Hudson, P. J. Shaw, and I. D. Williams, “Developing a systematic method for extraction of microplastics in soils,” *Anal. Methods*, vol. 13, no. 14, pp. 1695–1705, 2021, doi: 10.1039/D0AY02086A.

[68] A. Bottone, J. Boily, A. Shchukarev, P. L. Andersson, and J. Klaminder, “Sodium hypochlorite as an oxidizing agent for removal of soil organic matter before microplastics analyses,” *J. Environ. Qual.*, vol. 51, no. 1, pp. 112–122, Jan. 2022, doi: 10.1002/jeq2.20321.

[69] J. J. Pignatello, E. Oliveros, and A. MacKay, “Advanced Oxidation Processes for Organic Contaminant Destruction Based on the Fenton Reaction and Related Chemistry,” *Crit. Rev. Environ. Sci. Technol.*, vol. 36, no. 1, pp. 1–84, Jan. 2006, doi: 10.1080/10643380500326564.

[70] M. Pérez, F. Torrades, J. A. García-Hortal, X. Domènech, and J. Peral, “Removal of organic contaminants in paper pulp treatment effluents under Fenton and photo-Fenton conditions,” *Appl. Catal. B Environ.*, vol. 36, no. 1, pp. 63–74, Feb. 2002, doi: 10.1016/S0926-3373(01)00281-8.

[71] J. S. Hanvey, P. J. Lewis, J. L. Lavers, N. D. Crosbie, K. Pozo, and B. O. Clarke, “A review of analytical techniques for quantifying microplastics in sediments,” *Anal. Methods*, vol. 9, no. 9, pp. 1369–1383, 2017, doi: 10.1039/C6AY02707E.

[72] Z.-M. Wang, J. Wagner, S. Ghosal, G. Bedi, and S. Wall, “SEM/EDS and optical microscopy analyses of microplastics in ocean trawl and fish guts,” *Sci. Total Environ.*, vol. 603–604, pp. 616–626, Dec. 2017, doi: 10.1016/j.scitotenv.2017.06.047.

[73] L. Cabernard, L. Roscher, C. Lorenz, G. Gerdts, and S. Primpke, “Comparison of Raman and Fourier Transform Infrared Spectroscopy for the Quantification of Microplastics in the Aquatic Environment,” *Environ. Sci. Technol.*, vol. 52, no. 22, pp. 13279–13288, Nov. 2018, doi: 10.1021/acs.est.8b03438.

[74] C. Rathore, M. Saha, P. Gupta, M. Kumar, A. Naik, and J. De Boer, “Standardization of micro-FTIR methods and applicability for the detection and identification of microplastics in environmental matrices,” *Sci. Total Environ.*, vol. 888, p. 164157, Aug. 2023, doi: 10.1016/j.scitotenv.2023.164157.

[75] C. F. Araujo, M. M. Nolasco, A. M. P. Ribeiro, and P. J. A. Ribeiro-Claro, “Identification of microplastics using Raman spectroscopy: Latest developments and future prospects,” *Water Res.*, vol. 142, pp. 426–440, Oct. 2018, doi: 10.1016/j.watres.2018.05.060.

[76] N. Peez, M.-C. Janiska, and W. Imhof, “The first application of quantitative 1H NMR spectroscopy as a simple and fast method of identification and quantification of microplastic particles (PE, PET, and PS),” *Anal. Bioanal. Chem.*, vol. 411, no. 4, pp. 823–833, Feb. 2019, doi: 10.1007/s00216-018-1510-z.

[77] L. Hermabessiere *et al.*, “Optimization, performance, and application of a pyrolysis-GC/MS method for the identification of microplastics,” *Anal. Bioanal. Chem.*, vol. 410, no. 25, pp. 6663–6676, Oct. 2018, doi: 10.1007/s00216-018-1279-0.

[78] P. Pfohl *et al.*, “Microplastic extraction protocols can impact the polymer structure,” *Microplastics Nanoplastics*, vol. 1, no. 1, p. 8, Dec. 2021, doi: 10.1186/s43591-021-00009-9.

[79] W. Wohlleben *et al.*, “Fragmentation and Mineralization of a Compostable Aromatic–Aliphatic Polyester during Industrial Composting,” *Environ. Sci. Technol. Lett.*, vol. 10, no. 8, pp. 698–704, Aug. 2023, doi: 10.1021/acs.estlett.3c00394.

[80] J. Schindelin *et al.*, “Fiji: an open-source platform for biological-image analysis,” *Nat. Methods*, vol. 9, no. 7, pp. 676–682, Jul. 2012, doi: 10.1038/nmeth.2019.

[81] R Core Team, *R: A Language and Environment for Statistical Computing*. (2024). R Foundation for Statistical Computing. [Online]. Available: https://www.R-project.org/

[82] C. K. Duesterberg, S. E. Mylon, and T. D. Waite, “pH Effects on Iron-Catalyzed Oxidation using Fenton’s Reagent,” *Environ. Sci. Technol.*, vol. 42, no. 22, pp. 8522–8527, Nov. 2008, doi: 10.1021/es801720d.

[83] LECO Corporation, “RC612,” LECO Corporation. Accessed: Sep. 04, 2024. [Online]. Available: https://www.leco.com/products/multiphase-determination/

[84] J. A. Zazo, G. Pliego, S. Blasco, J. A. Casas, and J. J. Rodriguez, “Intensification of the Fenton Process by Increasing the Temperature,” *Ind. Eng. Chem. Res.*, vol. 50, no. 2, pp. 866–870, Jan. 2011, doi: 10.1021/ie101963k.

[85] A. Goi and M. Trapido, “Degradation of polycyclic aromatic hydrocarbons in soil: The fenton reagent versus ozonation,” *Environ. Technol.*, vol. 25, no. 2, pp. 155–164, Feb. 2004, doi: 10.1080/09593330409355448.

[86] I. Satilmis and W. Schrader, “Studying the Fenton treatment of polycyclic aromatic compounds in a highly contaminated soil with different modifiers by high

resolution mass spectrometry," *J. Hazard. Mater. Adv.*, vol. 8, p. 100200, Nov. 2022, doi: 10.1016/j.hazadv.2022.100200.

[87] K. Kaiser and G. Guggenberger, "Mineral surfaces and soil organic matter," *Eur. J. Soil Sci.*, vol. 54, no. 2, pp. 219–236, Jun. 2003, doi: 10.1046/j.1365-2389.2003.00544.x.

[88] M. Hubbe, M. Nazhad, and C. Sanchez, "Composting as a way to convert cellulosic biomass and organic waste into high-value soil amendments: A review," *BioResources*, vol. 5, no. 4, pp. 2808–2854, Nov. 2010, doi: 10.15376/biores.5.4.2808-2854.

[89] W. Yao *et al.*, "Promoting lignin exploitability in compost: A cooperative microbial depolymerization mechanism," *Process Saf. Environ. Prot.*, vol. 174, pp. 856–868, Jun. 2023, doi: 10.1016/j.psep.2023.05.003.

[90] J. Zhao, Y. Zhang, H. Cong, C. Zhang, and J. Wu, "Quantifying the contribution of lignin to humic acid structures during composting," *Chem. Eng. J.*, vol. 492, p. 152204, Jul. 2024, doi: 10.1016/j.cej.2024.152204.

[91] A. V. Barker, "Composition and Uses of Compost," in *Agricultural Uses of By-Products and Wastes*, vol. 668, in ACS Symposium Series, no. 668, vol. 668. , American Chemical Society, 1997, pp. 140–162. doi: 10.1021/bk-1997-0668.ch010.

[92] F. Büks, G. Kayser, A. Zieger, F. Lang, and M. Kaupenjohann, "Particles under stress: ultrasonication causes size and recovery rate artifacts with soil-derived POM but not with microplastics," *Biogeosciences*, vol. 18, no. 1, pp. 159–167, Jan. 2021, doi: 10.5194/bg-18-159-2021.

[93] G. McKay, M. M. Dong, J. L. Kleinman, S. P. Mezyk, and F. L. Rosario-Ortiz, "Temperature Dependence of the Reaction between the Hydroxyl Radical and Organic Matter," *Environ. Sci. Technol.*, vol. 45, no. 16, pp. 6932–6937, Aug. 2011, doi: 10.1021/es201363j.

Appendix

List of Figures

Figure 1: Major types of plastics based on their origin and degradability. 1
Figure 3: Chemical structure and process of conversion of lactic acid to polylactic acid. Created with Marvin (https://chemaxon.com). 6
Figure 4: Chemical structure and synthesis of PBAT. Created with Marvin (https://chemaxon.com). 7
Figure 5: Overview of the composting process with typical organic waste sources in Europe. 10
Figure 6: Overview of various Fenton oxidation procedures. a: Dropwise addition, b: General procedure with direct addition, c: Fenton oxidation in an ultrasound bath. 20
Figure 7: The images illustrate the general Fenton oxidation and filter procedure. They demonstrate the following stages: sonication of the compost sample in Milli-Q (a), samples during Fenton oxidation (b), filtering of the Fenton-compost solution (c), addition of HCl onto filters after filtering the Fenton-compost solution (d), and the solid compost residue after drying (e). 21
Figure 8: Determination of the combustible fraction of native compost. Native compost in ceramic vessel before combustion (a), high-temperature oven (b), native compost in ceramic vessel after combustion placed in a desiccator (c) 25
Figure 9: Measurement of TOC values. Fenton/compost residue preparation (a). Samples after combustion and TOC measurement, note: the reddish samples are from the maximum removal tests and clearly show the increased iron content (b). 26
Figure 10: Polymer stability test. Fenton oxidation (a). Testing of different filters (b). Polymer particles on filters in the untreated state, after sonication, after Fenton oxidation (c). Digital optical microscopy of a filter containing particles treated with Fenton, preliminary step for size distribution analysis (d). 28
Figure 11: Left: Original microscope image, right: outline drawing of particles created with Fiji [73]. 29
Figure 12: Effect of Fenton reaction conditions on mass removal efficiency. The plot shows average mass removal from triplicate experiments. H_2O_2 (35%) and $FeSO_4$ (0.05M) were added every 30 minutes (five additions) to 1 g compost in 40 mL Milli-Q water. 34
Figure 13: Comparison of the results of mass removal after Fenton treatment between the Wohlleben et al. (2023) method and the optimised Fenton protocol. 35
Figure 14: Comparison of mass removal efficiency across different addition methods. Dropwise addition (a): 75 mL H_2O_2 (time independent) and 30 mL $FeSO_4$. Dropwise addition (b): 5x10 mL H_2O_2 and 5x5 mL $FeSO_4$. Direct addition (Optimised Fenton protocol), ultrasound bath, and dropwise addition (c) use

5x10 mL H_2O_2 (35%) and 5x10 mL $FeSO_4$ (0.05M) every 30 minutes. Dropwise addition (d): 5x20 mL H_2O_2 and 5x10 mL $FeSO_4$ every 30 minutes. 36
Figure 15: White particles floating on the surface of the residual NaOCl-compost solution during filtration. 38
Figure 16: Carbon intensity comparison between a representative sample for Native Compost, the Optimised Fenton Procedure and the Wohlleben et al. (2023) method 39
Figure 17: Comparison between the total organic carbon of native compost before and after organic matrix removal methods (Optimised Fenton protocol and Wohlleben et al. (2023) method). 41
Figure 18: Histograms of the size distribution of the polymer particles. Comparison between pristine condition and after either sonication only, Fenton only or complete treatment (Fenton and sonication). 47

List of Tables

Table 1: Overview of the tested organic matrix removal protocols, summarising the various reagent concentrations and the key procedural conditions (see Chapter 4.1 for details). For $FeSO_4$, 0.05 M corresponds to approximately 15 mg/mL and 0.07 M to 20 mg/mL. 22
Table 2: Results of the combustible fraction of native compost. Mass removal was calculated based on the difference in mass before and after combustion 42
Table 3: Percentiles (D10, median D50, D90 with Area converted to diameter) describing the size distribution of the PLA and PBAT particles in pristine status, after sonication only, after Optimised Fenton treatment only and after the complete procedure (sonication and Fenton). Results are presented as percentiles (D10, D50 and D90) ± bootstrapped SD. 44

List of Abbreviations

AWG = Abfallwirtschaftsgesetz

BDO = 1,4-butanediol

BioAbfV = Bioabfall Verordnung

BGK = Bundesgütegemeinschaft Kompost

CO_2 = Carbon dioxide

DMT = Dimethyl terephthalate

Fe = Iron

Fe^{2+} = Ferrous iron

Fe^{3+} = Ferric iron

$FeCl_2$ = Iron(II) chloride

$Fe(OH)_3$ = Ferric hydroxide

$FeSO_4$ x 7 H_2O = Iron (II) sulphate heptahydrate

FTIR = Fourier Transform Infrared Spectroscopy

GC-MS = Gas chromatography-mass spectrometry

H^+ = Proton

H_2O = Water

H_2O_2 = Hydrogen Peroxide

HCl = Hydrochloric acid

KrWG = Kreislaufwirtschaftsgesetz

LOI = Loss-on-ignition

mm = Millimeter

Milli-Q = Milli-Q water

MPs = Microplastics

NaOCl = Sodium Hypochlorite

NMR = Nuclear Magnetic Resonance Spectroscopy

O_2 = Oxygen

OH• = Hydroxyl radicals

OH^- = Hydroxide ion

PBAT = Polybutylene adipate terephthalate

PE = Polyethylene

PET = Polyethylene terephthalate

PLA = Polylactic acid

PLLA = Poly-L-lactide

PP = Polypropylene

PS = Polystyrene

SD = Standard deviation

SDGs = Sustainable Development Goals

SEM = Scanning Electron Microscopy

SiC = Silicon carbide

TC = Total carbon

TEM = Transmission Electron Microscopy

TIC = Total inorganic carbon

TOC = Total organic carbon

TPA = Terephthalic acid

Tween 20 = Polysorbate 20

WWTPs = Wastewater treatment plants

µm = Micrometer

Supplementary Information

Table S 1: Statistical results of the particle analysis with RStudio.

Metric	PLA Pristine vs. PLA Sonication	PLA Pristine vs. PLA Fenton	PLA Pristine vs. PLA Complete	PBAT Pristine vs. PBAT Sonication	PBAT Pristine vs. PBAT Fenton	PBAT Pristine vs. PBAT Complete
Descriptive Statistics						
Count (Group 1, Group 2)	97, 92	97, 106	97, 102	118, 92	118, 106	118, 82
Mean (µm) (Group 1, Group 2)	149, 153	149, 147	149, 137	125, 135	125, 120	125, 108
SD (µm) (Group 1, Group 2)	70.50, 87.10	70.50, 84.30	70.50, 87.30	63.10, 66.80	63.10, 60.50	63.10, 75.20
Median (µm) (Group 1, Group 2)	141, 129	141, 115	141, 98	108, 124	108, 101	108, 81
IQR (µm) (Group 1, Group 2)	114, 117	114, 152	114, 117	92, 89	92, 85	92, 56
Shapiro-Wilk Normality Test						
W-statistic (Group 1)	0.93533	0.93533	0.93533	0.88342	0.88342	0.88342
p-value (Group 1)	1.293×10^{-4}	1.293×10^{-4}	1.293×10^{-4}	3.730×10^{-8}	3.730×10^{-8}	3.730×10^{-8}
W-statistic (Group 2)	0.88239	0.87792	0.82857	0.9016	0.87956	0.66306
p-value (Group 2)	5.68×10^{-7}	7.60×10^{-8}	1.59×10^{-9}	3.86×10^{-6}	8.94×10^{-8}	2.01×10^{-12}
Percentiles						
D10 (µm) (Group 1, Group 2)	64.85, 65.22	64.85, 61.46	64.85, 59.63	61.46, 62.63	61.46, 60.09	61.46, 58.26
D50 (µm) (Group 1, Group 2)	140.54, 128.91	140.54, 115.24	140.54, 98.02	108.11, 123.84	108.11, 101.09	108.11, 80.70
D90 (µm) (Group 1, Group 2)	252.21, 296.05	252.21, 263.57	252.21, 253.24	221.15, 236.76	221.15, 213.29	221.15, 184.59
SD of Percentiles						
SD(D10) (Group 1, Group 2)	2.60, 3.66	2.60, 1.11	2.60, 1.67	1.42, 2.93	1.42, 1.29	1.42, 1.14
SD(D50) (Group 1, Group 2)	11.05, 8.81	11.05, 16.09	11.05, 10.46	6.46, 8.53	6.46, 7.43	6.46, 5.31
SD(D90) (Group 1, Group 2)	10.54, 21.80	10.54, 12.45	10.54, 12.75	12.57, 18.81	12.57, 12.16	12.57, 36.29
Mann-Whitney U Test						
Test Statistic (W)	4551	5496	5707	4880	6533	5993
p-value	0.8139	0.3965	0.0614	0.2102	0.5652	0.0041
Alternative Hypothesis	No difference	No difference	No difference	No difference	No difference	Significant difference
Rank-Biserial Correlation						
Effect Size	0.0172	0.0596	0.133	0.0866	0.0385	0.203
Magnitude	Small	Small	Small	Small	Small	Small
Conf. Low	0.0027	0.0025	0.0100	0.0047	0.0029	0.0700
Conf. High	0.17	0.2	0.26	0.21	0.17	0.33

Table S 2: Overview of organic matrix removal protocols. Unless stated otherwise, doses were added directly with a 30-minute interval between additions.

Experimental setup	Initial conditions		Dose 1		Dose 2		Dose 3		Dose 4		Dose 5		Final conditions		Filter mass [g]	Final mass [g]	Mass removal (%)
	T (°C)	pH	T (°C)	pH	T (°C)	pH	T (°C)	pH	T (°C)	pH	T (°C)	pH	T (°C)	pH			
5 x 15 mL H_2O_2 (35%); 5 x 10 mL $FeSO_4$ (0.05 M)	24.7	7.81	25.9	3.40	35.0	2.43	35.4	2.42	45.1	2.38	37.7	2.59	-	-	0.24	1.10	14
5 x 15 mL H_2O_2 (35%) (35%); 1 x 20 mL $FeSO_4$ (0.05 M) (at start)	22.0	7.82	23.9	2.72	25.3	2.42	25.3	2.22	23.4	2.19	23.4	2.22	-	-	0.24	1.16	8
	24.7	7.75	24.9	2.63	26.4	2.40	25.7	2.24	23.8	2.17	23.4	2.14	-	-	0.24	1.17	7
	24.0	7.79	25.2	2.65	27.5	2.44	25.3	2.32	24.2	2.20	23.8	2.14	-	-	0.23	1.17	6
5 x 10 mL H_2O_2 (35%); 5 x 10 mL $FeSO_4$ (0.05 M)	22.9	7.76	22.0	4.08	22.3	2.63	25.7	2.28	34.1	2.17	46.0	2.41	-	-	0.24	1.03	21
	24.0	7.94	23.2	3.82	22.3	2.55	25.0	2.30	34.9	2.16	44.9	2.29	-	-	0.24	1.05	19
	27.9	7.84	25.5	4.45	22.7	2.96	23.9	2.44	29.6	2.27	34.4	2.24	-	-	0.25	0.99	26
5 x 15 mL H_2O_2 (35%); 5 x 10 mL $FeSO_4$ (0.05 M)	21.6	3.54	22.3	2.40	24.6	2.03	26.1	1.90	32.5	1.84	74.2	2.25	20.0	2.26	0.25	1.06	19
	22.0	4.40	22.6	2.70	24.6	2.18	26.4	1.90	29.6	1.85	79.9	2.22	20.6	2.20	0.24	1.09	15
	23.2	3.72	22.1	2.63	24.2	2.19	26.8	1.97	28.7	1.92	72.1	2.27	20.7	2.24	0.24	1.14	10
5 x 25 mL H_2O_2 (35%); 5 x 10 mL $FeSO_4$ (0.05 M)	24.0	4.76	23.4	2.64	24.6	1.94	25.7	1.82	28.0	1.67	31.1	1.64	27.0	1.88	0.25	1.03	22
	23.6	3.97	23.1	2.51	24.6	1.86	26.0	1.68	27.7	1.61	31.1	1.59	23.4	2.17	0.24	1.14	10
	25.8	4.68	23.5	2.77	24.6	1.95	26.0	1.74	27.7	1.65	31.4	1.63	25.2	1.80	0.25	1.06	19
5 x 25 mL H_2O_2 (35%); 5 x 25 mL $FeSO_4$ (0.05 M) (heated to 50 °C)	50.0	3.86	55.0	1.89	82.0	2.03	56.7	2.13	58.1	2.14	54.6	2.12	23.8	2.09	0.25	1.24	1
	50.0	3.60	56.0	1.91	65.0	2.09	61.5	2.11	52.1	2.14	51.2	2.16	23.4	2.12	0.24	1.23	1
	50.0	3.85	67.0	1.85	60.2	2.12	63.7	2.13	54.8	2.15	58.9	2.11	22.7	2.09	0.24	1.18	6
5 x 5 mL H_2O_2 (35%); 5 x 5 mL $FeSO_4$ (0.05 M)	23.0	3.98	21.6	3.02	21.5	2.55	22.3	2.26	22.3	2.08	23.8	1.98	21.8	1.89	0.24	1.05	19
	23.0	3.84	22.4	3.01	21.9	2.55	22.3	2.21	22.3	2.14	23.8	2.04	21.8	1.92	0.25	1.02	23
	23.1	3.95	21.9	3.10	22.0	2.57	22.3	2.21	22.3	2.07	23.8	2.01	21.8	1.91	0.25	1.06	19
5 x 25 mL H_2O_2 (35%); 5 x 25 mL $FeSO_4$ (0.05 M)	22.1	3.23	25.4	2.11	26.8	1.97	74.0	2.15	44.1	2.69	43.5	2.19	21.2	2.52	0.24	1.16	8
	22.4	3.51	24.3	2.21	26.9	1.97	84.0	2.06	43.4	2.65	42.3	2.41	21.2	2.53	0.25	1.16	9
	23.6	3.56	25.2	2.21	27.1	1.97	83.7	2.05	42.1	2.74	43.0	2.72	22.4	2.52	0.24	1.16	8
5 x 15 mL H_2O_2 (35%); 1 x 25 mL $FeSO_4$ (0.05 M) (at start)	24.1	3.74	24.7	2.23	25.7	2.84	23.5	3.24	23.4	3.40	22.7	2.90	21.4	3.28	0.24	1.06	18
	25.2	3.91	25.8	2.22	25.4	2.43	23.9	3.19	23.4	3.40	22.7	3.29	22.2	2.96	0.24	1.02	22
	26.5	3.67	27.2	2.34	25.3	2.05	23.9	3.25	23.4	2.83	23.1	3.35	21.8	2.91	0.24	1.03	21
5 x 10 mL H_2O_2 (35%); 5 x 5 mL $FeSO_4$ (0.05 M); 5 mL HCl 2M onto filters	22.4	3.39	22.4	2.96	21.9	2.35	22.3	2.01	23.1	2.01	23.4	1.86	20.7	2.51	0.24	1.04	20
	23.2	3.86	23.6	3.01	21.5	2.44	22.3	2.21	22.7	1.95	23.1	1.87	21.1	2.60	0.24	1.03	21
	26.5	3.98	25.4	3.01	21.5	2.48	21.9	2.89	22.7	1.85	22.7	1.93	21.5	2.34	0.24	1.01	23
dropwise addition of 75 mL H_2O_2 (35%); 1 x 30 mL $FeSO_4$ (0.07 M) (at start); 5 mL HCl 2M onto filters	22.4	3.70	25.3	2.10	28.7	1.62	26.0	1.42	-	-	-	-	22.0	2.90	0.24	1.05	19
	22.7	3.73	29.7	1.93	28.4	1.58	26.4	1.47	-	-	-	-	22.7	3.29	0.24	1.04	20
	-	-	28.3	1.96	31.4	1.82	26.4	1.59	-	-	-	-	23.2	3.35	0.24	1.10	14
dropwise addition of 5 x 10 mL H_2O_2 (35%); 5 x 5 mL $FeSO_4$ (0.07 M); 5 mL HCl 2M onto filters	24.0	3.35	22.3	2.57	23.1	2.14	23.1	1.80	23.8	1.72	26.7	1.65	23.2	1.62	0.24	0.96	28
	24.8	3.25	22.8	2.44	23.5	2.01	23.4	1.86	24.2	1.74	26.0	1.70	23.9	1.66	0.24	1.03	21
	27.2	3.69	23.6	2.70	23.1	2.01	23.5	1.93	24.6	1.70	24.6	1.71	23.1	2.03	0.25	0.85	40
dropwise addition of 5 x 20 mL H_2O_2 (35%); 5 x 10 mL $FeSO_4$ (0.07 M); 5 mL HCl 2M onto filters	23.6	3.38	23.1	2.76	25.7	1.89	31.7	1.64	88.2	2.01	55.0	3.03	20.8	2.43	0.24	0.85	39
	25.1	3.70	23.9	2.29	26.4	1.92	31.4	1.67	82.5	2.07	54.6	3.06	21.6	2.39	0.24	0.89	35
	26.2	3.80	24.7	3.10	26.8	1.85	29.3	1.67	78.2	2.47	55.5	3.03	21.6	2.45	0.24	0.88	36
dropwise addition of 5 x 10 mL H_2O_2 (35%); 5 x 10 mL $FeSO_4$ (0.07 M); 5 mL HCl 2M onto filters	26.2	3.39	23.9	2.24	26.1	1.86	27.4	1.84	35.9	1.86	53.6	2.03	22.0	2.30	0.24	0.85	39
	21.6	3.43	22.3	2.15	25.0	1.98	27.4	1.83	33.4	1.91	52.6	2.06	20.7	2.69	0.24	0.91	33
	27.4	3.21	35.2	2.03	48.3	1.80	52.1	1.96	44.2	2.06	46.3	2.08	20.4	2.42	0.24	0.91	33
5 x 10 mL H_2O_2 (35%); 5 x 10 mL $FeSO_4$ (0.07 M); 5 mL HCl 2M onto filters	25.6	3.54	26.0	2.33	25.6	2.55	30.9	1.84	54.0	2.11	39.8	2.21	21.5	2.42	0.24	0.85	39
	27.7	3.99	27.0	2.40	25.9	2.24	30.3	1.84	55.8	2.09	41.8	2.21	21.9	2.36	0.24	0.81	43
	31.3	3.66	29.4	2.36	26.2	2.03	29.0	1.93	51.7	2.32	40.1	2.33	21.9	2.35	0.24	0.86	38
Ultrasound bath: 5 x 10 mL H_2O_2 (35%); 5 x 10 mL $FeSO_4$ (0.07 M); 5 mL HCl 2M onto filters	27.5	2.50	33.4	2.47	49.1	2.11	33.4	2.21	48.0	2.17	54.0	2.07	22.5	2.21	0.24	0.91	33
5 x 25 mL H_2O_2 (35%); 5 x 25 mL $FeSO_4$ (0.07 M); 5 mL HCl 2M onto filters	30.8	2.16	35.2	2.01	82.8	1.86	49.4	1.96	47.9	2.00	47.2	2.02	22.7	2.00	0.24	1.05	19
	26.8	2.99	34.2	2.03	81.3	1.85	50.3	1.96	48.2	1.95	48.7	2.00	22.6	2.21	0.24	1.26	0
	24.5	2.93	29.4	2.11	79.5	1.84	49.6	1.89	46.4	2.02	49.2	1.96	23.5	1.96	0.24	1.22	2
Wohlleben et al. (2023) protocol; 5 mL HCl 2M onto filters	22.8	3.62	22.8	2.99	22.0	2.56	23.3	1.96	23.3	1.67	24.1	1.74	27.3	1.90	0.24	0.88	36
	22.8	2.78	22.8	3.01	22.0	2.33	22.9	2.01	23.3	1.80	24.1	1.78	27.1	1.78	0.25	0.87	36
	23.6	3.77	23.2	2.86	22.4	2.26	22.8	1.95	22.4	1.61	24.1	1.71	26.7	1.71	0.24	0.82	42
1M (upper row) and 2M (lower row) NaOCl 1:5 ratio; direct addition onto dry compost	23.7	12.16	22.1	11.76	22.0	10.54	20.7	9.89	20.7	9.64	20.1	9.33	21.6	9.29	0.24	0.94	30
	27.1	8.38	26.0	8.04	23.3	7.72	22.1	7.74	21.2	7.90	21.1	7.94	21.1	7.94	0.24	0.89	35
5 x 10 mL H_2O_2 (35%); 5 x 10 mL $FeSO_4$ (0.05 M); 5 mL HCl 2M onto filters	22.8	3.88	-	-	-	-	-	-	-	-	-	-	20.9	2.48	0.13	0.84	29
	23.6	3.98	-	-	-	-	-	-	-	-	-	-	21.4	2.45	0.13	0.75	38
	24.0	3.82	-	-	-	-	-	-	-	-	-	-	21.0	2.51	0.13	0.74	39
	24.9	3.89	-	-	-	-	-	-	-	-	-	-	20.3	2.46	0.13	0.79	34
	26.2	3.92	25.5	2.62	23.1	2.21	25.1	2.14	48.6	2.23	31.8	2.20	20.2	2.59	0.13	0.78	35
5 x 10 mL H_2O_2 (35%); 5 x 10 mL $FeSO_4$ (0.05 M); 5 mL HCl 2M onto filters	23.6	2.31	24.0	2.45	24.9	2.19	29.4	2.01	46.3	2.25	36.9	2.32	21.6	2.72	0.13	0.80	33
	23.8	2.38	-	-	-	-	-	-	-	-	-	-	22.0	2.51	0.13	0.82	31
	24.9	2.94	-	-	-	-	-	-	-	-	-	-	21.9	2.43	0.14	0.76	37

Table S 3: Total organic carbon measurements of Native Compost and Fenton treatment procedures (Optimised Fenton protocol, Wohlleben et al. (2023) method).

Sample	TOC (%)
Native Compost	10.57
Native Compost	16.81
Native Compost	11.28
Native Compost	14.35
Native Compost	13.11
Native Compost	14.69
Native Compost	13.50
Native Compost	11.99
Native Compost	14.31
Native Compost	16.83
Native Compost	15.20
Wohlleben et al. (2023) method	1.94
Wohlleben et al. (2023) method	2.80
Wohlleben et al. (2023) method	1.51
Wohlleben et al. (2023) method	1.94
Optimised Fenton protocol	4.69
Optimised Fenton protocol	3.77
Optimised Fenton protocol	1.94
Optimised Fenton protocol	3.31
Optimised Fenton protocol	0.97
Optimised Fenton protocol	1.06
Optimised Fenton protocol	3.01
Optimised Fenton protocol	2.68
Optimised Fenton protocol	3.14
Optimised Fenton protocol	3.08
Optimised Fenton protocol	2.11
Optimised Fenton protocol	2.09
Optimised Fenton protocol	2.42
Optimised Fenton protocol	3.24
Optimised Fenton protocol	2.14
Optimised Fenton protocol	2.44
Optimised Fenton protocol	1.31
Optimised Fenton protocol	1.17
Optimised Fenton protocol	2.41
Optimised Fenton protocol	2.69
Optimised Fenton protocol	1.71
Optimised Fenton protocol	1.95
Average Native Compost	**13.88 ± 2.05**
Average Wohlleben et al. (2023) method	**2.05 ± 0.54**
Average Optimised Fenton protocol	**2.42 ± 0.92**

Table S 4: Weight [g] of ceramic bowls + 1,00 g compost before combustion (a), after combustion (b) and calculated weight removal (c).

a [g]	b [g]	c [g]
24.87	24.57	0.30
25.96	25.56	0.40
24.95	24.63	0.32
27.21	26.80	0.41
32.81	32.45	0.36
Average		**0.36 ± 0.04**

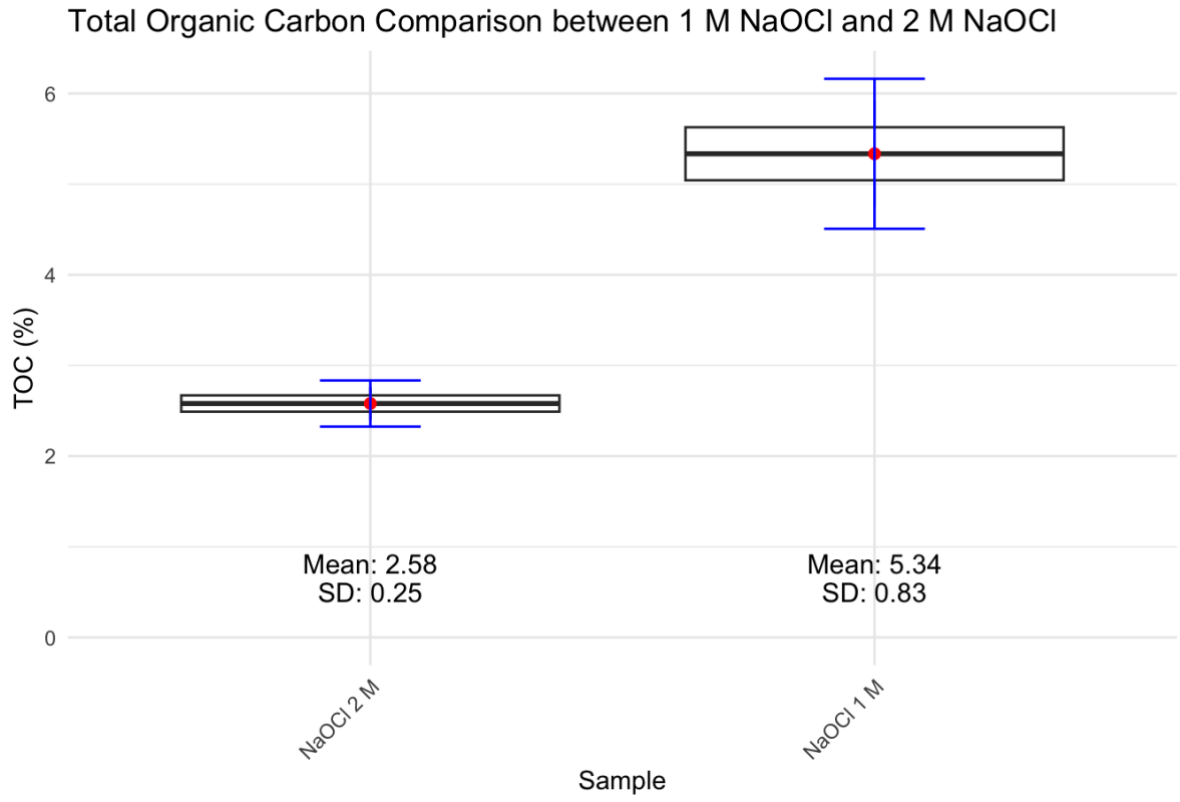

Figure S 1: Total Organic Carbon of NaOCl treated compost samples.

RStudio Scripts

1. Particle analysis with PLA pristine vs. PLA complete treatment as an example. All R Scripts for the polymer particle analysis were performed in the same way.

```
# Install and load necessary libraries
install.packages("dplyr")
install.packages("ggplot2")
install.packages("readr")
install.packages("rstatix")
install.packages("rcompanion")

library(dplyr)
library(ggplot2)
library(readr)
library(rstatix)
library(rcompanion)

# Load data: choose import dataset, excel file: Results_overview_sonicati
on, then the sheet J59_J60 PLA
data <- Results_overview_sonication

# Convert the 'Sample' column to a factor
data$Sample <- as.factor(data$Sample)

# Rename the sample names (use only for histograms, boxplots)
data <- data %>%
  mutate(Sample = recode(Sample,
                         "J59" = "PLA pristine",
                         "J60" = "PLA sonication"))

# Convert Area to Diameter (in micrometres)
data <- data %>%
  mutate(Diameter = 2 * sqrt(Area / pi))  # Convert area to diameter

# Create a new column for Diameter bins (50 µm intervals), with the last
bin being ≥450 µm
data <- data %>%
  mutate(Diameter_bin = cut(Diameter,
                            breaks = c(seq(0, 450, by = 50), Inf),  # Adj
ust for the last bin to include values ≥450
                            include.lowest = TRUE,
                            right = FALSE,
                            labels = c(paste0(seq(0, 400, by = 50), "-",
seq(50, 450, by = 50)), "≥450")))

# Descriptive statistics for Diameter
descriptive_stats <- data %>%
  group_by(Sample) %>%
  summarise(
```

```r
    count = n(),
    mean = mean(Diameter, na.rm = TRUE),
    sd = sd(Diameter, na.rm = TRUE),
    median = median(Diameter, na.rm = TRUE),
    IQR = IQR(Diameter, na.rm = TRUE)
  )

print(descriptive_stats)

# Visualize the data
# Boxplot of Diameter
ggplot(data, aes(x = Sample, y = Diameter)) +
  geom_boxplot() +
  labs(title = "Boxplot of Diameter by Sample", x = "Sample", y = express
ion("Diameter (" * mu * m * ")"))

# Histogram of Diameter (Percentage per Size Class) with summarized bins
(50 µm)
ggplot(data, aes(x = Diameter_bin, fill = Sample)) +
  geom_bar(position = "dodge", aes(y = (..count..)/sum(..count..)*100)) +
  # Normalize to percentage
  labs(title = "Histogram of Diameter by Sample", x = "Diameter (µm)", y
= "Percentage of Particles per Size Class") +
  scale_fill_manual(values = c("blue", "red")) +
  theme(axis.text.x = element_text(angle = 45, hjust = 1))  # Rotate x-ax
is labels for better clarity

# Normality test (Shapiro-Wilk test)
shapiro_test_J59 <- shapiro.test(data$Diameter[data$Sample == "PLA pristi
ne"])
shapiro_test_J60 <- shapiro.test(data$Diameter[data$Sample == "PLA sonica
tion"])

print(shapiro_test_J59)
print(shapiro_test_J60)

# Inferential statistics
# Mann-Whitney U Test
mann_whitney_test <- wilcox.test(Diameter ~ Sample, data = data)

# Print test results
print(mann_whitney_test)

# Calculate rank-biserial correlation
rank_biserial_corr <- wilcox_effsize(Diameter ~ Sample, data = data, ci =
 TRUE, conf.level = 0.95)

# Print rank-biserial correlation
print(rank_biserial_corr)

# Calculate percentiles for each sample group
percentiles <- data %>%
  group_by(Sample) %>%
  summarise(
```

```
    D10 = quantile(Diameter, 0.10, na.rm = TRUE),
    D50 = quantile(Diameter, 0.50, na.rm = TRUE),
    D90 = quantile(Diameter, 0.90, na.rm = TRUE)
  )

# Print the results
print(percentiles)

# Function to calculate percentiles
calculate_percentiles <- function(data) {
  return(quantile(data$Diameter, probs = c(0.1, 0.5, 0.9), na.rm = TRUE))
}

# Bootstrapping function
bootstrap_percentiles <- function(data, n_bootstrap = 1000) {
  bootstrap_results <- replicate(n_bootstrap, {
    resampled_data <- data %>% sample_frac(replace = TRUE)
    calculate_percentiles(resampled_data)
  })
  return(bootstrap_results)
}

# Calculate SDs for each sample
calculate_sd <- function(data, sample_label) {
  data_sample <- data %>% filter(Sample == sample_label)
  set.seed(123)  # For reproducibility
  bootstrap_results <- bootstrap_percentiles(data_sample)

  # Calculate standard deviation for D10, D50, and D90
  sd_D10 <- sd(bootstrap_results[1, ])
  sd_D50 <- sd(bootstrap_results[2, ])
  sd_D90 <- sd(bootstrap_results[3, ])

  return(c(sd_D10, sd_D50, sd_D90))
}

# Perform bootstrapping for each sample
sd_J59 <- calculate_sd(data, "PLA pristine")
sd_J60 <- calculate_sd(data, "PLA sonication")

# Print results
print("PLA pristine SDs: ")
print(sd_J59)
print("PLA sonication SDs: ")
print(sd_J60)
```

2. TOC Analysis Fenton Protocols

```
# Load necessary libraries
library(dplyr)
library(ggplot2)
```

```r
# data input
data <- data.frame(
  Sample = c("Optimised Fenton protocol", "Optimised Fenton protocol", "O
ptimised Fenton protocol", "Optimised Fenton protocol",
             "Optimised Fenton protocol", "Optimised Fenton protocol", "O
ptimised Fenton protocol", "Optimised Fenton protocol",
             "Optimised Fenton protocol", "Optimised Fenton protocol", "O
ptimised Fenton protocol", "Optimised Fenton protocol",
             "Optimised Fenton protocol", "Optimised Fenton protocol", "O
ptimised Fenton protocol", "Optimised Fenton protocol",
             "Optimised Fenton protocol", "Optimised Fenton protocol", "O
ptimised Fenton protocol", "Optimised Fenton protocol",
             "Optimised Fenton protocol", "Optimised Fenton protocol", "N
ative Compost", "Native Compost", "Native Compost",
             "Native Compost", "Native Compost", "Native Compost", "Nativ
e Compost", "Native Compost", "Native Compost",
             "Native Compost", "Native Compost", "Wohlleben et al. (2023)
 method", "Wohlleben et al. (2023) method",
             "Wohlleben et al. (2023) method", "Wohlleben et al. (2023) m
ethod"),
  Value = c(4.69, 3.77, 1.94, 3.31, 0.97, 1.06, 3.01, 2.68, 3.14, 3.08, 2
.11, 2.09, 2.42, 3.24, 2.14, 2.44, 1.31, 1.17, 2.41, 2.69,
            1.71, 1.95, 10.57, 16.81, 11.28, 14.35, 13.11, 14.69, 13.50,
11.99, 14.31, 16.83, 15.20, 1.94, 2.80, 1.51, 1.94)
)

# Sort the Sample factor levels
data$Sample <- factor(data$Sample, levels = c("Native Compost", "Wohllebe
n et al. (2023) method", "Optimised Fenton protocol"))

# Calculate mean and standard deviation for each sample group
stats <- data %>%
  group_by(Sample) %>%
  summarise(
    Mean = mean(Value),
    SD = sd(Value)
  )

# Create the boxplot
p <- ggplot(data, aes(x = Sample, y = Value)) +
  geom_boxplot() +
  stat_summary(fun = mean, geom = "point", shape = 20, size = 3, color =
"red") +
  geom_errorbar(data = stats, aes(x = Sample, ymin = Mean - SD, ymax = Me
an + SD, y = Mean), width = 0.2, color = "blue") +
  geom_text(data = stats, aes(x = Sample, y = max(data$Value) + 2, label
= paste("Mean:", round(Mean, 2))), hjust = -0.2) +
  geom_text(data = stats, aes(x = Sample, y = max(data$Value) + 1, label
= paste("SD:", round(SD, 2))), hjust = -0.2) +
  labs(x = "Sample", y = "TOC (%)") +
  theme_minimal() +
  theme(axis.text.x = element_text(angle = 45, hjust = 1))
```

```r
# Display the plot
print(p)
```

3. Carbon Intensity Comparison

```r
# Load the necessary libraries
library(ggplot2)
library(dplyr)

# Data 'J70', 'J50_2', and 'Native_Compost_Blank2' excel files (exported
as csv files directly from the LECO, and then converted to excel) are use
d for this comparison
# Combine datasets into one data frame with new names
data <- bind_rows(
  J70 %>% mutate(dataset = "Optimised Fenton Procedure"),
  J50_2_ %>% mutate(dataset = "Wohlleben et al. (2023) method"),
  Native_Compost_Blank2 %>% mutate(dataset = "Native Compost")
)

# Calculate total carbon intensity
data$total_intensity <- data$CO2LO + data$CO2HI

# Create the plot
p <- ggplot(data, aes(x = `CO2LO (sec)`, group = dataset)) +
  # Plot carbon intensity for each dataset
  geom_line(aes(y = total_intensity, color = dataset), size = 0.05) +
  geom_point(aes(y = total_intensity, color = dataset), size = 0.5) +

  # Add labels
  labs(
    x = "Time (seconds)",
    y = "Intensity"
  ) +

  # Add a secondary y-axis for temperature
  scale_y_continuous(
    name = "Intensity",
    sec.axis = sec_axis(~ . / 6.36, name = "Temperature (°C)")  # Using c
alculated scaling factor
  ) +

  # Plot temperature on the same graph using secondary y-axis
  geom_line(aes(y = `Temperature (∞C)` * 6.36, linetype = "Temperature"),
 color = "black", size = 0.3) + # Adjust scaling factor to match the axes

  # Customise colour and theme
  scale_color_manual(values = c("Optimised Fenton Procedure" = "blue",
                                "Wohlleben et al. (2023) method" = "green
",
                                "Native Compost" = "red")) +
```

```r
  # Add a manual linetype for the temperature line in the legend
  scale_linetype_manual(values = c("Temperature" = "dashed")) +

  # Remove the word "dataset" from the legend
  guides(color = guide_legend(title = NULL),
         linetype = guide_legend(title = NULL)) +

  # Customise the theme
  theme_minimal() +
  theme(
    legend.position = "bottom",
    plot.title = element_blank(),  # Remove the title completely
    plot.margin = margin(10, 10, 10, 10),  # Adjust plot margins
    panel.background = element_rect(fill = "white", color = NA),  # Ensur
e white background
    plot.background = element_rect(fill = "white", color = NA)    # Ensur
e plot background is white
  )

# Display the plot
p

# Save the plot
ggsave("my_plot_zoom.png", plot = p, width = 12, height = 8, dpi = 300)
# Adjust dimensions as needed
```

4. Fenton Conditions Comparison

```r
# Data preparation
data <- data.frame(
  Fenton_Conditions = c(
    "25ml H2O2, 25ml FeSO4", "25ml H2O2, 25ml FeSO4", "25ml H2O2, 25ml Fe
SO4",
    "15 ml H2O2, 10 ml FeSO4", "15 ml H2O2, 10 ml FeSO4", "15 ml H2O2, 10
 ml FeSO4",
    "5 ml H2O2, 5 ml FeSO4", "5 ml H2O2, 5 ml FeSO4", "5 ml H2O2, 5 ml Fe
SO4",
    "10 ml H2O2, 5 ml FeSO4", "10 ml H2O2, 5 ml FeSO4", "10 ml H2O2, 5 ml
 FeSO4",
    "10ml H2O2, 10ml FeSO4", "10ml H2O2, 10ml FeSO4", "10ml H2O2, 10ml Fe
SO4",
    "10ml H2O2, 10ml FeSO4", "10ml H2O2, 10ml FeSO4", "10ml H2O2, 10ml Fe
SO4",
    "10ml H2O2, 10ml FeSO4", "10ml H2O2, 10ml FeSO4", "10ml H2O2, 10ml Fe
SO4",
    "10ml H2O2, 10ml FeSO4", "10ml H2O2, 10ml FeSO4"
  ),
  Mass_Removal = c(
    19, 0, 2,
    19, 15, 10,
    19, 23, 19,
```

```
    20, 21, 23,
    39, 43, 38, 29, 38, 39,
    34, 35, 33, 31, 37
  )
)

# Calculate averages and standard deviations
summary_stats <- aggregate(Mass_Removal ~ Fenton_Conditions, data, functi
on(x) c(mean = mean(x), sd = sd(x)))
summary_stats <- do.call(data.frame, summary_stats)
names(summary_stats) <- c("Fenton_Conditions", "Mean", "SD")

# Sort by average Mass Removal
summary_stats <- summary_stats[order(summary_stats$Mean), ]

# Boxplot preparation
library(ggplot2)

# Update Fenton_Conditions labels with subscript notation for H₂O₂ and Fe
SO₄
data$Fenton_Conditions <- factor(data$Fenton_Conditions, levels = summary
_stats$Fenton_Conditions)
labels <- c(
  expression("25 ml H"[2]*"O"[2]*", 25 ml FeSO"[4]),
  expression("15 ml H"[2]*"O"[2]*", 10 ml FeSO"[4]),
  expression("5 ml H"[2]*"O"[2]*", 5 ml FeSO"[4]),
  expression("10 ml H"[2]*"O"[2]*", 5 ml FeSO"[4]),
  expression("10 ml H"[2]*"O"[2]*", 10 ml FeSO"[4])
)

# Create the boxplot
ggplot(data, aes(x = Fenton_Conditions, y = Mass_Removal)) +
  geom_boxplot() +
  scale_x_discrete(labels = labels) +
  labs(
       x = "Fenton Conditions",
       y = "Mass Removal (%)") +
  theme_minimal() +
  theme(axis.text.x = element_text(angle = 45, hjust = 1))
```

5. Addition Method Comparison

```
# Load necessary library
library(ggplot2)
library(dplyr)

# Create the dataset
data <- data.frame(
  Method = c("Direct addition", "Direct addition", "Direct addition", "Di
rect addition", "Direct addition",
             "Direct addition", "Direct addition", "Direct addition", "Di
```

```
rect addition", "Direct addition",
             "Direct addition", "Dropwise addition (a)", "Dropwise additi
on (a)", "Dropwise addition (a)",
             "Dropwise addition (b)", "Dropwise addition (b)", "Dropwise
addition (b)",
             "Dropwise addition (d)", "Dropwise addition (d)", "Dropwise
addition (d)",
             "Dropwise addition (c)", "Dropwise addition (c)", "Dropwise
addition (c)",
             "Ultrasound bath"),
  MassRemoval = c(39, 43, 38, 29, 38, 39, 34, 35, 33, 31, 37, 19, 20, 14,
 28, 21, 40, 39, 35, 36, 39, 33, 33, 33)
)

# Specify the desired order for the methods, placing "Direct addition" la
st
data$Method <- factor(data$Method, levels = c(
  "Dropwise addition (a)", "Dropwise addition (b)", "Dropwise addition (c
)",
  "Dropwise addition (d)", "Ultrasound bath", "Direct addition"
))

# Create the boxplot
ggplot(data, aes(x = Method, y = MassRemoval)) +
  geom_boxplot(aes(color = Method), fill = "white", outlier.shape = NA) +
  scale_color_manual(
    values = c("Direct addition" = "blue", "Dropwise addition (a)" = "bla
ck",
               "Dropwise addition (b)" = "black", "Dropwise addition (c)"
 = "black",
               "Dropwise addition (d)" = "black", "Ultrasound bath" = "bl
ack")
  ) +
  labs(
    x = "Method",
    y = "Mass Removal (%)"
  ) +
  theme_minimal() +
  theme(
    axis.text.x = element_text(angle = 45, hjust = 1),
    legend.position = "none"
  )
```

6. TOC Analysis NaOCl Protocol

```
# Load necessary libraries
library(dplyr)
library(ggplot2)

# Input data with updated sample names
data <- data.frame(
```

```
  Sample = c("NaOCl 2 M", "NaOCl 2 M",
             "NaOCl 1 M", "NaOCl 1 M"),
  Value = c(2.40, 2.76, 5.92, 4.75)
)

# Sort the Sample factor levels
data$Sample <- factor(data$Sample, levels = c("NaOCl 2 M", "NaOCl 1 M"))

# Calculate mean and standard deviation for each sample group
stats <- data %>%
  group_by(Sample) %>%
  summarise(
    Mean = mean(Value),
    SD = sd(Value)
  )

# Create the boxplot
p <- ggplot(data, aes(x = Sample, y = Value)) +
  geom_boxplot() +
  stat_summary(fun = mean, geom = "point", shape = 20, size = 3, color =
"red") +
  geom_errorbar(data = stats, aes(x = Sample, ymin = Mean - SD, ymax = Me
an + SD, y = Mean),
                width = 0.2, color = "blue") +
  geom_text(data = stats, aes(x = Sample, y = max(data$Value) + 0.5, labe
l = paste("Mean:", round(Mean, 2))), hjust = -0.2) +
  geom_text(data = stats, aes(x = Sample, y = max(data$Value) + 0.3, labe
l = paste("SD:", round(SD, 2))), hjust = -0.2) +
  labs(x = "Sample", y = "TOC (%)") +
  theme_minimal() +
  theme(axis.text.x = element_text(angle = 45, hjust = 1))

# Display the plot
print(p)
```

NaOCl Molarity Calculation and Dilution

Molarity of 12.5% NaOCl:

- Density: 1.206 g/mL

$$M = \frac{mol\ \text{NaOCl}}{L\ \text{of solution}}$$

$$\frac{100\ g\ \text{solution}}{1} \times \frac{1\ mL}{1.206\ g} \times \frac{1\ L}{1000\ mL} = 0.08297874\ L$$

$$\frac{12.5\ g\ \text{NaOCl}}{1} \times \frac{1\ mol\ \text{NaOCl}}{74.44\ g\ \text{NaOCl}} \times \frac{1}{0.08297874\ L} = 2.0236569\ M$$

Preparation of 100 mL 1 M NaOCl from a 2.0236569 M stock solution:

$$M1 \times V1 = M2 \times V2$$

- $M1 = 2.0236569\ M$
- $V1 = \frac{1\ M \times 100\ mL}{2.0236569\ M} = 49.42\ mL$
- $M2 = 1\ M$
- $V2 = 100\ mL$

$$49.42\ mL \text{ of } 2.0236569\ M\ \text{NaOCl} + 50.58\ mL \text{ of MilliQ} = 100\ mL \text{ of } 1\ M\ \text{NaOCl}$$

Calibration of the Carbon Analyser

Before quantification, the instrument must be calibrated through blank and drift corrections. This requires heating the instrument to 1000 °C and maintaining that temperature for one hour to have a stable detection for all the components (some catalysers require high temperatures for certain yields and stability). During this time, three samples each of a synthetic low-carbon standard (1% carbon, approximately 85 mg) and a calcium carbonate standard (12% carbon, approximately 77 mg) are weighed. For the blank correction, at least three blank measurements are taken. The software automatically performs the correction using the selected results. Next, the low- and high-carbon standards are analysed. The results from these standards are then used by the software to perform the drift correction, ensuring accurate measurement of the samples.

Determination of the Combustible Fraction

Mass difference before and after combustion:

$$\Delta m = (m_{\text{vessel}} + m_{\text{compost}}) - m_{\text{after}}$$

Mass removal efficiency (η):

$$\eta = \left(\frac{\Delta m}{m_{\text{compost}}}\right) \times 100\%$$

- $m_{\text{vessel}} =$ Mass of the ceramic vessel before combustion
- $m_{\text{compost}} =$ 1 gram of compost
- $m_{\text{after}} =$ Mass of the ceramic vessel with the compost in it after combustion